

1

Supplementary information

2 **$\alpha\beta,\alpha'\beta'$ -Diepoxyketones are Mechanism-Based Inhibitors of Nucleophilic Cysteine Enzymes**

3 Mariska de Munnik^a, Jasper Lithgow^a, Lennart Brewitz^a, Kirsten E. Christensen^b, Robert Bates^c, Beatriz
4 Rodriguez-Miquel^c, and Christopher J. Schofield^{*a}

5 ^a Chemistry Research Laboratory, Department of Chemistry and the Ineos Oxford Institute of
6 Antimicrobial Research, University of Oxford, 12 Mansfield Road, Oxford, OX1 3TA, United Kingdom.

7 ^b Chemical Crystallography, Chemistry Research Laboratory, Department of Chemistry, University of
8 Oxford, 12 Mansfield Road, Oxford, OX1 3TA, United Kingdom.

9 ^c Tres Cantos Medicines Development Campus GlaxoSmithKline, Calle Severo Ochoa 2, Tres Cantos,
10 Madrid, Spain.

11 * Email: christopher.schofield@chem.ox.ac.uk

12 **Experimental details**

13 **Materials**

14 Recombinant Ldt_{Mt2} was produced in *Escherichia coli* and purified (>95% purity by SDS-PAGE analysis)
15 as reported.¹ Recombinant SARS-CoV-2 M^{pro} was produced by Eidarus Salah and purified as reported.²
16 Probe 1 (2-(6-(((2,4-dinitrophenyl)sulfonyl)oxy)-3-oxo-3H-xanthen-9-yl)benzoic acid) and FC-5 was
17 synthesised as reported.^{3, 4} DEK **1** was initially obtained from the GSK compound collection in
18 enantiopure form, and then synthesised as a single diastereomer as outlined below. Epoxide **12** was
19 purchased from Enamine in diastereomerically pure form. All reagents for the preparation of **1** and **4**
20 – **11** were from commercial sources (Sigma-Aldrich, Inc.; Fluorochem Ltd; Alfa Aesar; Manchester
21 Organics) and were used as received. Purifications by column chromatography were performed using
22 an automated Biotage® Selekt instrument (wavelengths monitored: 254 and 280 nm) equipped with
23 pre-packed Biotage® Sfär Silica D chromatography cartridges. Thin layer chromatography (TLC) was
24 carried out using Merck Silica gel 60 F254 TLC plates. Melting points (m.p.) were determined using a
25 Stuart SMP-40 automated melting point apparatus. Infrared (IR) spectroscopy was performed using a
26 Bruker Tensor-27 Fourier transform infrared (FT-IR) spectrometer. High-resolution mass spectrometry
27 (HRMS) was performed using electro-spray ionization (ESI) mass spectrometry (MS) in the positive
28 ionisation mode employing a Thermo Scientific Exactive mass spectrometer (ThermoFisher Scientific).
29 Nuclear magnetic resonance (NMR) spectroscopy was performed using a Bruker AVANCE AVIIIHD 400
30 instrument.

31 **Inhibition studies**

32 Ldt_{Mt2} fluorogenic assays were performed as described.³ Ldt_{Mt2} (100 nM) was incubated with varying
33 concentrations of a potential inhibitor (400 μM – 20.3 nM) for 10 min in the assay buffer (50 mM
34 HEPES, pH 7.2, 0.01% (v/v) Triton X-100) and then assayed using Probe 1 (25 μM).

35 SARS-CoV-2 M^{pro} inhibition assays were performed as described.⁵ M^{pro} (150 nM) was incubated with
36 varying concentrations of inhibitor (100 μM – 1.7 nM) for 15 min in assay buffer (20 mM HEPES, pH
37 7.5, 50 mM NaCl) and then assayed using a 37mer peptide as the substrate
38 (ALNDFSNSGSDVLYQPPQTSITSAVLQSGFRKMAFPS-NH₂, 2 μM).

39 BlaC fluorogenic assays were performed as described.^{4, 6} BlaC (14 nM) was incubated with varying
40 concentrations of inhibitor (400 μM – 20.3 nM) for 10 min in assay buffer (100 mM sodium phosphate
41 pH 7.5, 0.01% (v/v) Triton X-100) and then assayed using FC5 (10 μM).

42 The 'intrinsic' thiol reactivity (k_{chem}) was determined as described.⁶ *L*-Glutathione (500 nM) was
43 incubated with varying concentrations of inhibitor (400 μM – 20.3 nM) and Probe 1 (10 μM) for 15 h
44 in assay buffer (50 mM HEPES, pH 7.2, 0.01% (v/v) Triton X-100).

45 The second-order rate constant of covalent target inactivation (k_{inact}/K_i) was determined as described.⁶
46 Ldt_{Mt2} (100 nM) was incubated with varying concentrations of inhibitor (400 μM – 20.3 nM) and Probe
47 1 (10 μM) for 3.5 h in assay buffer (50 mM HEPES, pH 7.2, 0.01% (v/v) Triton X-100).

48 **Protein observed SPE-MS assays**

49 Protein-observed SPE-MS experiments with Ldt_{Mt2} were performed as described.⁶ Ldt_{Mt2} (1 μM) in 50
50 mM tris, pH 7.5 was incubated with an inhibitor (20 μM) at room temperature.

51 SARS-CoV-2 M^{pro} protein-observed SPE-MS experiments were performed as described.^{2, 5}

52 **X-ray crystallography**

53 Recombinant Ldt_{Mt2} ($\Delta 1-55$; with the N-terminal His₆-Tag removed, in 50 mM tris, pH 8.0, 100 mM NaCl)
54 was crystallised using sitting drop vapor diffusion at 4 °C, according to a reported procedure.⁶ The
55 inhibitor was introduced to the crystals through soaking (1.5 mM, 24 h), after which time the crystals
56 were cryocooled and stored in liquid nitrogen. Datasets were collected using the MX beamline I03 at
57 the Diamond Light Source synchrotron (Harwell, United Kingdom). Structures were solved by
58 molecular replacement using Phaser⁷, using PDB entry 6RRM⁸ as the search model. Alternating cycles
59 of refinement using PHENIX⁹ and manual model building using COOT¹⁰ were performed until R_{work} and
60 R_{free} converged. Data collection and refinement statistics can be found in Table S2. Ligands were
61 visualised by $mF_o - DF_c$ polder OMIT map.¹¹

62 Single crystal X-ray diffraction data were collected for **1** at 150 K using a (Rigaku) Oxford Diffraction
63 SuperNova diffractometer and CrysAlisPro. The structure was solved using 'Superflip'¹² before
64 refinement with CRYSTALS^{13, 14} as described in the SI (CIF). The crystallographic data have been
65 deposited with the Cambridge Crystallographic Data Centre (CCDC 2262059), and copies of these data
66 can be obtained free of charge from The Cambridge Crystallographic Data Centre via
67 www.ccdc.cam.ac.uk/data_request/cif.

68 **Preparation of recombinant BlaC protein**

69 A codon-optimised synthetic gene (GeneArt, Thermo Fisher Scientific) encoding for BlaC $\Delta 1-40$ was
70 amplified and cloned into the expression vector pCold using Sal1-HF (New England BioLabs) and Not1-
71 HF (New England BioLabs) digestion and ligation using T4 DNA ligase (New England BioLabs) according
72 to the manufacturer's protocol. The ampicillin resistance gene of the vector was exchanged for the

73 kanamycin resistance gene using Gibson Assembly,¹⁵ and transformed with *Escherichia coli* BL21(DE3).
74 An overnight culture of *E. coli* BL21(DE3) pCold-BlaC Δ 1-40 was grown at 37 °C at 180 rpm in 2xTY
75 media (with 50 μ g/mL kanamycin). This culture was used to inoculate fresh 2xTY media containing 50
76 μ g/mL kanamycin (1% (v/v)), which was grown at 37 °C at 180 rpm to OD₆₀₀ of 0.6. Then, 0.5 mM
77 Isopropyl β -D-thiogalactopyranoside (IPTG) was added and the culture was incubated at 18 °C at 180
78 rpm for an additional 16 h. Cells were collected by centrifugation (11,000 x g, 8 min), and stored at -80
79 °C.

80 The cell pellet was resuspended in HisTrap Buffer A (25 mM Tris-HCl pH 8.0, 500 mM NaCl, 0.5 mM
81 tris(2-carboxyethyl)phosphine) (TCEP), 5% (v/v) glycerol, 20 mM imidazole) in the presence of DNase
82 I, and lysed using a Continuous Flow Cell Disruptor (Constant Systems, 20 kpsi). The lysates were
83 centrifuged (32,000 x g, 20 min), passed through a 0.45 μ m filter, and loaded onto a 5 mL HisTrap
84 column (GE Life Sciences) that had been pre-equilibrated in HisTrap Buffer A. The column was washed
85 with HisTrap Buffer A, followed by a gradient running from 0 % to 100 % (v/v) HisTrap Buffer B (25 mM
86 Tris-HCl pH 8.0, 500 mM NaCl, 0.5 mM TCEP, 5% (v/v) glycerol, 250 mM imidazole). Fractions containing
87 BlaC (as observed by SDS-PAGE) were combined, the buffer was exchanged to HisTrap Buffer A, and
88 the HisTag was cleaved using recombinant 3C protease at 4 °C, over 12 h. The HisTag cleaved BlaC was
89 passed through a 5 mL HisTrap column (GE Life Sciences) and washed with HisTrap Buffer A. The BlaC
90 containing fractions (as observed by NanoDrop (Thermo Scientific) analysis) were concentrated and
91 loaded onto a 300 mL Superdex 75 column (GE Life Sciences) pre-equilibrated in gel filtration buffer
92 (25 mM Tris-HCl pH 8.0, 500 mM NaCl, 0.5 mM TCEP, 5% (v/v) glycerol). BlaC was eluted using the gel
93 filtration buffer. Fractions containing BlaC (as observed by SDS-PAGE) were combined, concentrated,
94 and frozen using liquid nitrogen. The identity and purity of BlaC was confirmed by mass spectrometry
95 (calculated mass 28740 Da, observed deconvoluted mass 28740 Da) and SDS-PAGE (>95% purity).

96 **Procedure for the synthesis of the diene precursors of 1 and 4-11 (General Procedure A)**

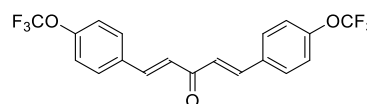
97 A modified literature procedure was followed to prepare the $\alpha\beta,\alpha'\beta'$ -dienone precursors of **1** and **4-**
98 **11**, i.e. **13-18**.¹⁶ To a neat solution of lithium perchlorate (LiClO₄) (20 mmol, 2 equiv.), benzaldehyde
99 (or a benzaldehyde derivative, as specified; 20 mmol, 2 equiv.), and the requisite ketone (10 mmol, 1
100 equiv.) was added triethylamine (Et₃N) (0.3 mL, 2 mmol, 0.1 equiv.). The mixture was stirred at room
101 temperature (rt) and the reaction progress was monitored by thin layer chromatography (TLC). Upon
102 completion of the reaction, a saturated aqueous ammonium chloride (NH₄Cl) solution was added, and
103 the resulting mixture was extracted with dichloromethane. The organic extracts were dried over
104 anhydrous sodium sulfate (Na₂SO₄) and concentrated under reduced pressure. The crude mixture was
105 purified by flash column chromatography.

106 **Procedure for the synthesis of DEKs 1 and 4-11 (General Procedure B)**

107 A modified literature procedure was followed to prepare $\alpha\beta,\alpha'\beta'$ -diepoxide ketones **1** and **4-11**.¹⁷ To a
108 stirred suspension of potassium fluoride supported on alumina (KF-Al₂O₃) (prepared as described¹⁸) in
109 *tert*-butyl hydroperoxide (^tBuOOH; 5.0-6.0 M in decane, 3.8 mL, ~21 mmol) under N₂ was added a
110 solution of the specified $\alpha\beta,\alpha'\beta'$ -dienone (2 mmol) in anhydrous acetonitrile (10 mL). The mixture was
111 stirred at rt, and the reaction progress was monitored by TLC. Upon completion of the reaction, the
112 mixture was filtered with a sintered funnel *in vacuo*. The filtrate was washed with brine and extracted
113 with ethyl acetate. The combined organic extracts were dried over anhydrous Na₂SO₄ and
114 concentrated *in vacuo*. The crude residue was purified by recrystallisation from ethanol to afford the
115 *trans/trans*- $\alpha\beta,\alpha'\beta'$ -diepoxide ketone.

116 **(1E,4E)-1,5-Bis(4-(trifluoromethoxy)phenyl)penta-1,4-dien-3-one (13)**

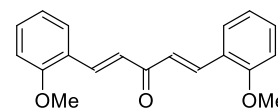
117 According to General Procedure A, diene **13** (2.37 g, 59%) was
118 obtained from 4-(trifluoromethoxy)benzaldehyde (3.80 g, 20 mmol)
119 and acetone (0.58 g, 10 mmol), following column chromatography
120 [50 g Sfär Silica D; 120 mL/min, 100% cyclohexane (2 CV (column volumes)), followed by a linear
121 gradient (12 CV): 0%→10% acetone in cyclohexane]. The analytical data for **13** were in agreement with
122 those reported.¹⁹



123 Yellow solid, m.p.: 119-121 °C; ¹H NMR (400 MHz, 300 K, CDCl₃): δ = 7.73 (d, *J* = 15.9 Hz, 2H), 7.70 –
124 7.61 (m, 4H), 7.27 (d, *J* = 8.0 Hz, 4H), 7.06 ppm (d, *J* = 16.0 Hz, 2H); ¹³C NMR (100 MHz, 300 K, CDCl₃): δ
125 = 188.2, 150.6 (q, *J* = 1.9 Hz), 141.8, 133.2, 129.8, 126.0, 121.2, 120.3 ppm (q, *J* = 258.2 Hz); ¹⁹F NMR
126 (376 MHz, 300 K, CDCl₃): δ = -57.8 ppm (s, 6F); IR (film): $\tilde{\nu}$ = 1651, 1580, 1508, 1263, 1214, 1190, 1164,
127 1109 cm⁻¹; HRMS (ESI): *m/z* calculated for C₁₉H₁₃O₃F₆ [M+H]⁺: 403.0763, found: 403.0760.

128 **(1E,4E)-1,5-Bis(2-methoxyphenyl)penta-1,4-dien-3-one (14)**

129 According to General Procedure A, diene **14** (2.29 g, 78%) was obtained from
130 2-methoxybenzaldehyde (2.72 g, 20 mmol) and acetone (0.58 g, 10 mmol),
131 following column chromatography [50 g Sfär Silica D; 120 mL/min, 100%
132 cyclohexane (2 CV), followed by a linear gradient (12 CV): 0%→20% acetone in cyclohexane]. The
133 analytical data for **14** were in agreement with those reported.²⁰



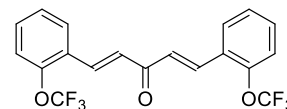
134 Yellow solid, m.p.: 125-128 °C; ¹H NMR (400 MHz, 300 K, CDCl₃): δ = 8.08 (d, *J* = 16.1 Hz, 2H), 7.62 (dd,
135 *J* = 7.7, 1.6 Hz, 2H), 7.36 (ddd, *J* = 8.3, 7.4, 1.7 Hz, 2H), 7.18 (d, *J* = 16.1 Hz, 2H), 6.98 (t, *J* = 7.5 Hz, 2H),
136 6.92 (d, *J* = 7.9 Hz, 2H), 3.90 ppm (s, 6H); ¹³C NMR (100 MHz, 300 K, CDCl₃): δ = 189.9, 158.5, 138.1,
137 131.5, 128.6, 126.1, 123.9, 120.6, 111.1, 55.4 ppm; IR (film): $\tilde{\nu}$ = 2838, 1666, 1647, 1612, 1598, 1573,

138 1487, 1464, 1437, 1336, 1296, 1274, 1246, 1184, 1163, 1106, 1049, 1026 cm⁻¹; HRMS (ESI): *m/z*
139 calculated for C₁₉H₁₉O₃ [M+H]⁺: 295.1329, found: 295.1330.

140

141 **(1*E*,4*E*)-1,5-Bis(2-(trifluoromethoxy)phenyl)penta-1,4-dien-3-one (15)**

142 According to General Procedure A, diene **15** (2.53 g, 63%) was obtained
143 from 2-(trifluoromethoxy)benzaldehyde (3.80 g, 20 mmol) and acetone
144 (0.58 g, 10 mmol), following column chromatography [100 g Sfär Silica D;

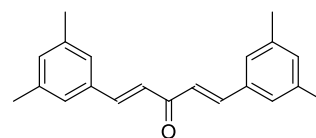


145 120 mL/min, 100% cyclohexane (2 CV), followed by a linear gradient (12 CV): 0%→10% acetone in
146 cyclohexane].

147 Yellow solid, m.p.: 75-78 °C; ¹H NMR (400 MHz, 300 K, CDCl₃): δ = 7.94 (d, *J* = 16.1 Hz, 2H), 7.74 (dd, *J* =
148 7.8, 1.7 Hz, 2H), 7.46 – 7.42 (m, 2H), 7.37 – 7.30 (m, 4H), 7.13 ppm (d, *J* = 16.1 Hz, 2H); ¹³C NMR (100
149 MHz, 300 K, CDCl₃): δ = 188.5, 147.9, 136.3, 131.5, 128.4, 128.0, 127.8, 127.1, 121.3, 120.5 ppm (q, *J* =
150 258.6 Hz); ¹⁹F NMR (376 MHz, 300 K, CDCl₃): δ = -57.3 ppm (s, 6F); IR (film) $\tilde{\nu}$ = 1660, 1623, 1603, 1487,
151 1457, 1334, 1248, 1210, 1170, 1098 cm⁻¹; HRMS (ESI): *m/z* calculated for C₁₉H₁₃O₃F₆ [M+H]⁺: 403.0763,
152 found: 403.0754.

153 **(1*E*,4*E*)-1,5-Bis(3,5-dimethylphenyl)penta-1,4-dien-3-one (16)**

154 According to General Procedure A, diene **16** (0.64 g, 22%) was obtained
155 from 3,5-dimethylbenzaldehyde (2.68 g, 20 mmol) and acetone (0.58 g,
156 10 mmol), following column chromatography [25 g Sfär Silica D; 80

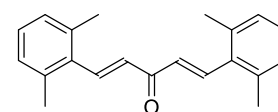


157 mL/min, 100% cyclohexane (2 CV), followed by a linear gradient (12 CV): 0%→15% acetone in
158 cyclohexane].

159 Yellow solid, m.p.: 109-111 °C; ¹H NMR (400 MHz, 300 K, CDCl₃): δ = 7.71 (d, *J* = 15.9 Hz, 2H), 7.27 –
160 7.25 (m, 4H), 7.13 – 7.05 (m, 4H), 2.38 ppm (s, 12H); ¹³C NMR (100 MHz, 300 K, CDCl₃): δ = 188.9, 143.3,
161 138.3, 134.7, 132.2, 126.2, 125.1, 21.1 ppm; IR (film): $\tilde{\nu}$ = 2980, 2918, 1652, 1620, 1604, 1439, 1341,
162 1287, 1255, 1188, 1161, 1105 cm⁻¹; HRMS (ESI): *m/z* calculated for C₂₁H₂₃O [M+H]⁺: 291.1743, found:
163 291.1743.

164 **(1*E*,4*E*)-1,5-Bis(2,6-dimethylphenyl)penta-1,4-dien-3-one (17)**

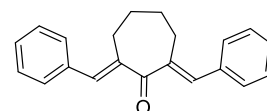
165 According to General Procedure A, diene **17** (0.20 g, 7%) was obtained from
166 2,6-dimethylbenzaldehyde (2.68 g, 20 mmol), and acetone (0.58 g, 10 mmol),
167 following recrystallisation from *n*-pentane.



168 Yellow solid, m.p.: 150-153 °C; ¹H NMR (400 MHz, 300 K, CDCl₃): δ = 7.92 (d, *J* = 16.3 Hz, 2H), 7.19 –
169 7.09 (m, 6H), 6.74 (d, *J* = 16.3 Hz, 2H), 2.43 ppm (s, 12H); ¹³C NMR (100 MHz, 300 K, CDCl₃): δ = 189.0,
170 142.1, 136.8, 134.4, 131.1, 128.4, 128.3, 21.1 ppm; IR (film): $\tilde{\nu}$ = 2981, 1650, 1625, 1591, 1467, 1446,
171 1382, 1355, 1291, 1192, 1165, 1004 cm⁻¹; HRMS (ESI): *m/z* calculated for C₂₁H₂₃O [M+H]⁺: 291.1743,
172 found: 291.1743.

173 **2,7-Di((*E*)-benzylidene)cycloheptan-1-one (18)**

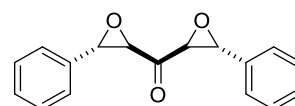
174 According to General Procedure A, diene **18** (0.78 g, 27%) was obtained from
175 benzaldehyde (2.12 g, 20 mmol) and cycloheptanone (1.12 g, 10 mmol)
176 following column chromatography [25 g Sfar Silica D; 80 mL/min, 100%
177 cyclohexane (2 CV), followed by a linear gradient (12 CV): 0%→10% acetone in cyclohexane]. The
178 analytical data for **18** were in agreement with those reported.^{21, 22}



179 Yellow solid, m.p.: 104-108 °C; ¹H NMR (400 MHz, 300 K, CDCl₃): δ = 7.53 – 7.33 (m, 12H), 2.78 – 2.70
180 (m, 4H), 2.04 – 1.99 ppm (m, 4H); ¹³C NMR (100 MHz, 300 K, CDCl₃): δ = 199.4, 141.7, 135.9, 135.6,
181 129.4, 128.4, 128.1, 28.8, 28.0 ppm; IR (film): $\tilde{\nu}$ = 2927, 1667, 1623, 1604, 1492, 1455, 1446, 1306,
182 1291, 1228, 1190, 1144, 1021 cm⁻¹; HRMS (ESI): *m/z* calculated for C₂₁H₂₁O [M+H]⁺: 289.1587, found:
183 289.1586.

184 **(*trans*-3-Phenyloxiran-2-yl)(*trans*-3-phenyloxiran-2-yl)methanone (1)**

185 According to General Procedure B, DEK **1** (180 mg, 35%) was obtained as a
186 single *trans,trans*-diastereomer from
187 (*1E,4E*)-1,5-diphenylpenta-1,4-dien-3-one¹⁶ (0.47 g, 2 mmol) following
188 recrystallisation from ethanol. The stereochemistry of **1** was assigned as *trans,trans* by X-ray diffraction
189 analysis of a single crystal obtained after recrystallisation (Table S4; CCDC 2262059). Note that the
190 analysis of the crude reaction mixture using ¹H NMR analysis indicated that two diastereomers are
191 formed during the reaction, one of which was assigned as the *trans,trans*-diastereomer; the other
192 diastereomer formed is likely the *cis,cis*-diastereomer (*cis,trans*-diastereomeric mixtures should
193 manifest in an additional set of signals for the epoxide protons and were not detected using ¹H NMR
194 analysis). Note that both the *trans,trans*-diastereomer and the *cis,cis*-diastereomer are *meso*-
195 compounds. The analytical data for **1** were in agreement with those reported.²³

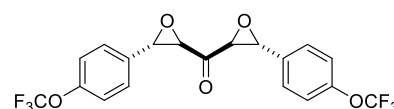


196 White crystals, m.p.: 119-120 °C. ¹H NMR (400 MHz, 300 K, CDCl₃): δ = 7.40 – 7.37 (m, 6H), 7.32 – 7.29
197 (m, 4H), 4.10 (d, *J* = 1.8 Hz, 2H), 3.81 ppm (d, *J* = 1.8 Hz, 2H); ¹³C NMR (100 MHz, 300 K, CDCl₃): δ =
198 199.2, 134.6, 129.3, 128.8, 125.8, 60.9, 59.0 ppm; IR (film): $\tilde{\nu}$ = 3062, 1721, 1458, 1428, 1410, 1117,
199 1084 cm⁻¹; HRMS (ESI): *m/z* calculated for C₁₇H₁₅O₃ [M+H]⁺: 267.1016, found: 267.1015.

200 Purification of the mother liquor obtained after recrystallization using column chromatography (10 g
201 Sfür Silica D; 40 mL/min, 100% cyclohexane (2 CV), followed by a linear gradient (12 CV): 0%→20%
202 ethyl acetate in cyclohexane) afforded a 3:1 mixture of *cis,cis:trans,trans*-**1** (37 mg, 7%) as an orange
203 oil. Note that *cis,cis*-enriched **1** appears to be an oil and not a solid like *trans,trans* **1**; as yet *cis,cis*-
204 enriched **1** has not been further purified by recrystallisation or trituration. By implication, subsequently
205 acquired diastereomerically pure $\alpha\beta,\alpha'\beta'$ -diepoxides obtained by crystallisation were *tentatively*
206 assigned as the *trans,trans*-diastereomers if they were obtained as pure solids. ¹H and ¹³C NMR signals
207 observed for *cis,cis*-enriched **1**: ¹H NMR (400 MHz, 300 K, CDCl₃): δ = 4.20 (d, *J* = 1.7 Hz, 2H), 3.74 ppm
208 (d, *J* = 1.7 Hz, 2H); ¹³C NMR(100 MHz, 300 K, CDCl₃): δ = 199.2, 134.5, 129.2, 128.7, 125.8, 60.3, 58.8
209 ppm.

210 **(*trans*-3-(4-(Trifluoromethoxy)phenyl)oxiran-2-yl)(*trans***
211 **3-(4-(trifluoromethoxy)phenyl)oxiran-2-yl)methanone (**4**)**

212 According to General Procedure B, DEK **4** (95 mg, 11%) was
213 obtained as a single diastereomer from diene **13** (0.81 g, 2 mmol)
214 following recrystallisation from ethanol. DEK **4** was *tentatively*

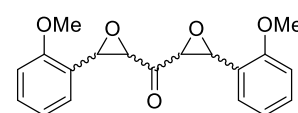


215 assigned as the *trans,trans*-diastereomer, in part because it was obtained as a solid after
216 recrystallization; *trans,trans*-**1** was a solid and its stereochemistry was assigned by crystallographic
217 analysis, whereas *cis,cis*-**1b** manifested as an oil.

218 White crystals, m.p.: 95-97 °C; ¹H NMR (400 MHz, 300 K, CDCl₃): δ = 7.38 – 7.34 (m, 4H), 7.28 – 7.25
219 (m, 4H), 4.16 (d, *J* = 1.8 Hz, 2H), 3.79 ppm (d, *J* = 1.8 Hz, 2H); ¹³C NMR (100 MHz, 300 K, CDCl₃): δ =
220 198.4, 149.9 (q, *J* = 1.9 Hz), 133.2, 127.3, 121.4, 120.6 (q, *J* = 257.8 Hz), 60.9, 58.1 ppm; ¹⁹F NMR (376
221 MHz, 300 K, CDCl₃): δ = -57.9 ppm (s, 6F); IR (film): $\tilde{\nu}$ = 1718, 1514, 1260, 1210, 1162 cm⁻¹; HRMS (ESI):
222 *m/z* calculated for C₁₉H₁₂O₅F₆Na [M+Na]⁺: 457.0481, found: 457.0481.

223 **(3-(2-Methoxyphenyl)oxiran-2-yl)(3-(2-methoxyphenyl)oxiran-2-yl)methanone (**5**)**

224 According to General Procedure B, DEK **5** (189 mg, 29%) was obtained from
225 diene **14** (0.59 g, 2 mmol) as a 2:1 mixture of diastereomers (likely the
226 *trans,trans*- and *cis,cis*-diastereomers) following column chromatography



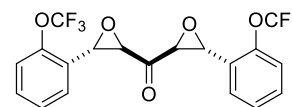
227 (10 g Sfür Silica D; 40 mL/min, 100% cyclohexane (2 CV), followed by a linear gradient (12 CV): 0%→20%
228 ethyl acetate in cyclohexane).

229 Analytical data for the ~2:1 mixture of diastereomers: ¹H NMR (400 MHz, 300 K, CDCl₃): δ = 7.36 – 7.31
230 (m, 6H), 7.23 – 7.18 (m, 6H), 7.00 – 6.91 (m, 12H), 4.51 (d, *J* = 1.8 Hz, 2H), 4.48 (d, *J* = 1.9 Hz, 4H), 3.90
231 (s, 12H), 3.88 (s, 6H), 3.74 (d, *J* = 1.8 Hz, 4H), 3.67 ppm (d, *J* = 1.8 Hz, 2H); ¹³C NMR (100 MHz, 300 K,

232 CDCl₃): δ = 200.1, 200.0, 158.3, 158.0, 129.8(4), 129.8, 125.3, 125.2, 123.6, 123.2, 120.8, 120.6, 110.4,
233 110.2, 60.3, 59.8, 55.4, 55.3(2), 55.3, 55.0 ppm; HRMS (ESI): m/z calculated for C₁₉H₁₉O₅ [M+H]⁺:
234 327.1227, found: 327.1227.

235 **(*trans*-3-(2-(Trifluoromethoxy)phenyl)oxiran-2-yl)(*trans*-**
236 **3-(2-(trifluoromethoxy)phenyl)oxiran-2-yl)methanone (6)**

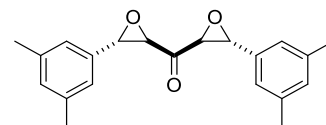
237 According to General Procedure B, DEK **6** (191 mg, 22%) was obtained as a
238 single diastereomer from diene **15** (0.81 g, 2 mmol) following
239 recrystallisation from ethanol. DEK **6** was *tentatively* assigned as the
240 *trans,trans*-diastereomer, in part because it was obtained as a solid after recrystallization (as described
241 above).



242 White crystals, m.p.: 136-139 °C. ¹H NMR (400 MHz, 300 K, CDCl₃): δ = 7.43 – 7.27 (m, 8H), 4.40 (d, J =
243 1.8 Hz, 2H), 3.71 ppm (d, J = 1.8 Hz, 2H); ¹³C NMR (100 MHz, 300 K, CDCl₃): δ = 198.0, 147.8, 130.2,
244 128.0, 127.5, 125.8, 121.1, 120.5 (q, J = 257.6 Hz), 60.1, 54.0 ppm; ¹⁹F NMR (376 MHz, 300 K, CDCl₃): δ
245 = -57.9 ppm (s, 6F); IR (film): $\tilde{\nu}$ = 1720, 1274, 1252, 1207, 1183, 1165, 1100, 1077 cm⁻¹; HRMS (ESI): m/z
246 calculated for C₁₉H₁₂O₅F₆Na [M+Na]⁺: 457.0481, found: 457.0479.

247 **(*trans*-3-(3,5-Dimethylphenyl)oxiran-2-yl)(*trans*-3-(3,5-dimethylphenyl)oxiran-2-yl)methanone (7)**

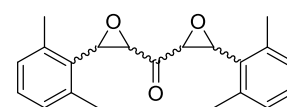
248 According to General Procedure B, DEK **7** (100 mg, 16%) was obtained as
249 a single diastereomer from diene **16** (0.59 g, 2 mmol) following
250 recrystallisation from ethanol. DEK **7** was *tentatively* assigned as the
251 *trans,trans*-diastereomer, in part because it was obtained as a solid after recrystallization (as described
252 above).



253 White crystals, m.p.: 124-128 °C. ¹H NMR (400 MHz, 300 K, CDCl₃): δ = 6.99 (s, 2H), 6.92 (s, 4H), 4.09
254 (d, J = 1.7 Hz, 2H), 3.69 (d, J = 1.7 Hz, 2H), 2.32 ppm (s, 12H); ¹³C NMR (100 MHz, 300 K, CDCl₃): δ =
255 199.5, 138.5, 134.4, 130.9, 123.5, 60.2, 58.9, 21.2 ppm; IR (film): $\tilde{\nu}$ = 2920, 1716, 1609, 1470, 1408,
256 1225, 1189, 1071, 1038 cm⁻¹; HRMS (ESI): m/z calculated for C₂₁H₂₂O₃Na [M+Na]⁺: 345.1461, found:
257 345.1463.

258 **(3-(2,6-Dimethylphenyl)oxiran-2-yl)(3-(2,6-dimethylphenyl)oxiran-2-yl)methanone (8)**

259 According to General Procedure B, DEK **8** (38 mg, 24%) was obtained from
260 diene **17** (145 mg, 0.5 mmol) as a 1.2:1 mixture of diastereomers (likely the
261 *trans,trans*- and *cis,cis*-diastereomers) following column chromatography (5

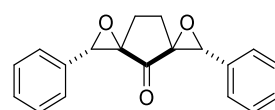


262 g Sfär Silica D; 18 mL/min, 100% cyclohexane (2 CV), followed by a linear gradient (12 CV): 0%→10%
263 ethyl acetate in cyclohexane).

264 Analytical data of the ~1.2:1 mixture of diastereomers: ^1H NMR (400 MHz, 300 K, CDCl_3): δ = 7.17 (t, J
265 = 7.6 Hz, 4H), 7.03 (d, J = 7.6 Hz, 8H), 4.32 (d, J = 2.0 Hz, 2H), 4.24 (d, J = 1.9 Hz, 2H), 3.78 (d, J = 2.1 Hz,
266 2H), 3.68 (d, J = 2.0 Hz, 2H), 2.43 (s, 12H), 2.42 ppm (s, 12H); ^{13}C NMR (100 MHz, 300 K, CDCl_3): δ =
267 201.9, 201.8(5), 137.2, 136.9, 131.5, 131.4(7), 128.5, 128.3, 128.2, 58.6, 58.3, 57.9, 57.8(6), 19.9, 19.7
268 ppm; HRMS (ESI): m/z calculated for $\text{C}_{21}\text{H}_{23}\text{O}_3$ $[\text{M}+\text{H}]^+$: 323.1642, found: 323.1642.

269 **(trans)-2,7-Diphenyl-1,6-dioxadispiro[2.1.2⁵.2³]nonan-4-one (9)**

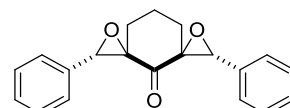
270 According to General Procedure B, DEK **9** (300 mg, 52%) was obtained as a
271 single diastereomer from 2,5-di((*E*)-benzylidene)cyclopentan-1-one¹⁶ (0.52 g,
272 2 mmol) without further purification. DEK **9** was *tentatively* assigned as the
273 *trans,trans*-diastereomer, in part because it was obtained as a solid.



274 White solid, m.p.: 115-118 °C. ^1H NMR (400 MHz, 300 K, CDCl_3): δ = 7.35 – 7.27 (m, 6H), 7.21 – 7.18 (m,
275 4H), 4.34 (s, 2H), 1.97 – 1.87 (m, 2H), 1.79 – 1.70 ppm (m, 2H); ^{13}C NMR (100 MHz, 300 K, CDCl_3): δ =
276 208.6, 133.4, 128.8, 128.5, 126.6, 66.1, 65.2, 19.9 ppm; IR (film): $\tilde{\nu}$ = 1762, 1410 cm^{-1} ; HRMS (ESI): m/z
277 calculated for $\text{C}_{19}\text{H}_{16}\text{O}_3\text{Na}$ $[\text{M}+\text{Na}]^+$: 315.0992, found: 315.0991.

278 **(trans)-2,7-Diphenyl-1,6-dioxadispiro[2.1.2⁵.2³]decan-4-one (10)**

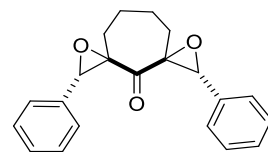
279 According to General Procedure B, DEK **10** (270 mg, 44%) was obtained as a
280 single diastereomer from 2,6-di((*E*)-benzylidene)cyclohexan-1-one¹⁶ (0.55 g,
281 2 mmol) without further purification. DEK **10** was *tentatively* assigned as the
282 *trans,trans*-diastereomer, in part because it was obtained as a solid.



283 White solid, m.p.: >230 °C (decomposition). ^1H NMR (400 MHz, 300 K, CDCl_3): δ = 7.44 – 7.30 (m, 10H),
284 4.15 (s, 2H), 2.15 – 2.07 (m, 2H), 1.65 – 1.58 (m, 3H), 1.25 – 1.11 ppm (m, 1H); ^{13}C NMR (100 MHz, 300
285 K, CDCl_3): δ = 203.1, 133.1, 128.6, 128.5, 126.6, 66.1, 65.5, 26.0, 19.4 ppm; IR (film): $\tilde{\nu}$ = 1716, 1453,
286 1407 cm^{-1} ; HRMS (ESI): m/z calculated for $\text{C}_{20}\text{H}_{18}\text{O}_3\text{Na}$ $[\text{M}+\text{Na}]^+$: 329.1148, found: 329.1148.

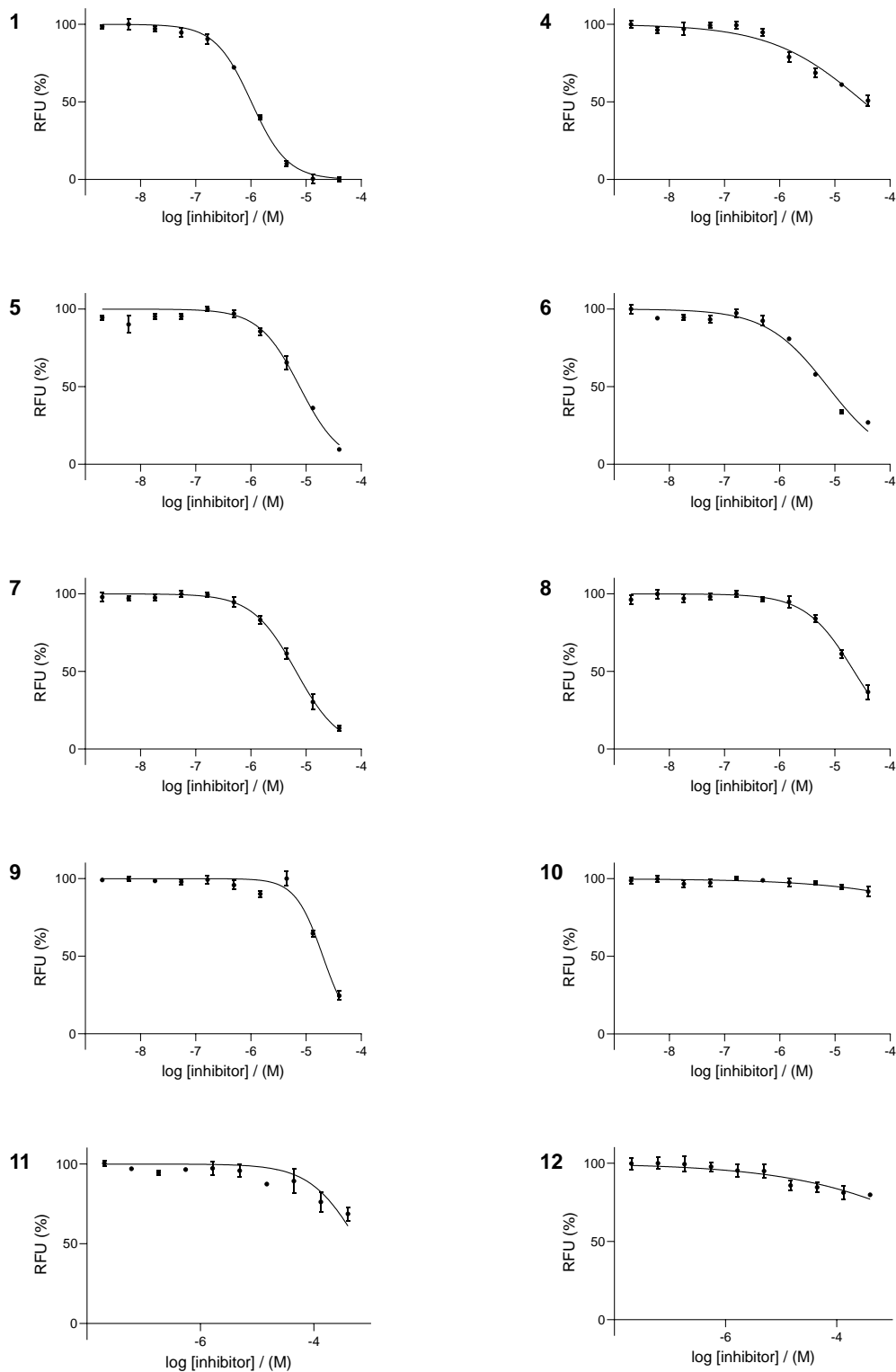
287 **(trans)-2,7-Diphenyl-1,6-dioxadispiro[2.1.2⁵.2³]undecan-4-one (11)**

288 According to General Procedure B, DEK **11** (260 mg, 41%) was obtained as a
289 single diastereomer from diene **18** (0.58 g, 2 mmol) without further
290 purification. DEK **11** was *tentatively* assigned as the *trans,trans*-diastereomer,
291 in part because it was obtained as a solid.



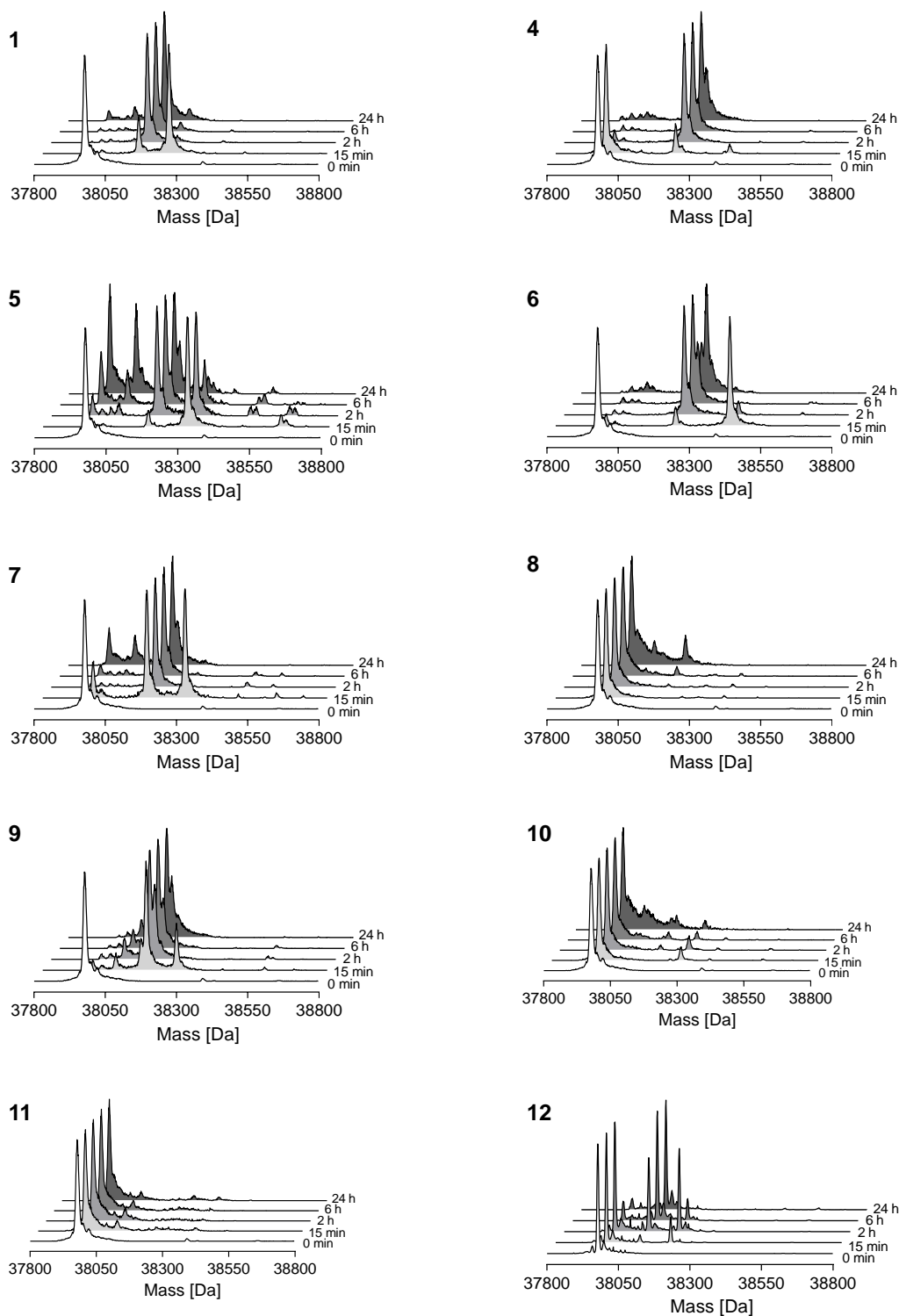
292 White solid, m.p.: 147-150 °C. ¹H NMR (400 MHz, 300 K, CDCl₃): δ = 7.40 – 7.32 (m, 10H), 4.23 (s, 2H),
293 1.90 – 1.79 (m, 4H), 1.49 – 1.46 (m, 2H), 1.35 – 1.31 ppm (m, 2H); ¹³C NMR (100 MHz, 300 K, CDCl₃): δ
294 = 203.6, 133.6, 128.4, 128.3, 126.6, 67.7, 63.9, 26.9, 24.4 ppm; IR (film): $\tilde{\nu}$ = 1718, 1454 cm⁻¹; HRMS
295 (ESI): *m/z* calculated for C₂₁H₂₀O₃Na [M+Na]⁺: 343.1305, found: 345.1306.

296



297

298 **Figure S1. Dose-response curves for the DEKs 1 and 4-11 and mono-epoxide ketone 12 with Ldt_{MT2} .** Inhibition
 299 assays were carried out using 100 nM Ldt_{MT2} and 25 μM Probe 1 with 10 min pre-incubation at room temperature
 300 in 50 mM HEPES, pH 7.2 with 0.01% (v/v) Triton X-100. Error bars represent standard deviation ($n=4$). Average
 301 pIC_{50} values and compound structures are given in Table S3.



302

303 **Figure S2. Protein observed SPE-MS analysis for the reaction of Ldt_{M2} with DEKs 1 and 4-11 and mono-epoxide**
 304 **ketone 12.** 1 μM Ldt_{M2} was incubated with the inhibitors (20 μM for **1** and **4 – 11**, 100 μM for **12**) at rt in 50 mM
 305 Tris, pH 7.5. Samples were analysed after the indicated times. Deconvoluted spectra, obtained using the
 306 maximum entropy algorithm in the MassHunter Workstation Qualitative Analysis B.07.00 program (Agilent), are
 307 shown. Mass shifts and assignments are given in Table S1.

308

309 **Table S1. Calculated and observed masses (Da) and mass shifts (Da) for protein-observed SPE-MS experiments**
 310 **with Ldt_{Mt2} and inhibitors 1 and 4-12, and their assignments.** Mass shifts are relative to unmodified Ldt_{Mt2}. The
 311 observed mass of the most abundant adduct at 24h is in blue. *Calculated mass for the fragmented adduct **3** (as
 312 shown in Figure 2). **Calculated mass for the unfragmented adduct **2** (as shown in Figure 2). Deconvoluted SPE-
 313 MS spectra are shown in Figure S2.

Compound	Calculated mass (Da)	Observed mass (Da)	Area (%) 15 min	Area (%) 24 h	Assignment
1		37944 (-34)	0.0	5.0	Dha
		37978 (+0)	2.0	0.0	Unmodified
	39139 (+161)*	38034 (+56)	0.0	5.9	Unassigned fragment ¹
	38245 (+267)**	38138 (+160)	23.3	82.0	Retro-aldol fragment (3)
		38245 (+267)	74.7	7.2	Unfragmented (2)
4		37944 (-34)	0.0	2.4	Dha
		37978 (+0)	76.5	0.0	Unmodified
	38223 (+245)*	38221 (+244)	18.1	97.6	Retro-aldol fragment (3)
	38413 (+435)**	38412 (+434)	5.41	0.0	Unfragmented (2)
5		37944 (-34)	0.0	30.4	Dha
		37978 (+0)	2.5	0.0	Unmodified
	38169 (+191)*	38035 (+57)	0.0	25.8	Unassigned fragment ¹
	38305 (+327)**	38169 (+191)	9.0	39.6	Retro-aldol fragment (3)
		38287 (+309)	0.0	4.22	N.D.
		38306 (+328)	77.9	0.0	Unfragmented (2)
6		37978 (+0)	7.2	2.6	Unmodified
	38223 (+245)*	38032 (+56 Da)	0.0	4.2	Fragment II ¹
	38413 (+435)**	38221 (+243)	11.6	93.2	Retro-aldol fragment (3)
		38413 (+435)	81.2	0.0	Unfragmented (2)
7		37944 (-34)	0.0	16.2	Dha
		37978 (+0)	11.5	0.0	Unmodified
	38167 (+189)*	38034 (+56)	0.0	13.5	Unassigned fragment ¹
	38210 (+232)**	38166 (+188)	43.7	70.3	Retro-aldol fragment (3)
		38301 (+232)	44.8	0.0	Unfragmented (2)
8		37978 (+0)	100.0	68.8	Unmodified
	38167 (+189)*	38058 (+80)	0.0	14.9	N.D.
	38210 (+232)**	38166 (+188)	0.0	16.3	Retro-aldol fragment (3)
9		37978 (+0)	3.3	0.0	Unmodified
	38165 (+187)*	38058 (+80)	6.9	9.1	N.D.
	38271 (+293)**	38163 (+185)²	68.8	90.9	Retro-aldol fragment (3)
		38271 (+293)	21.0	0.0	Unfragmented (2)
10	38179 (+201)*	37978 (+0)	100.0	90.2	Unmodified
	38285 (+307)**	38285 (+307)	0.0	9.8	Unfragmented (2)
11	38193 (+215)*	37978 (+0)	100.0	100.0	Unmodified
	38299 (+321)**				
12		37978 (+0)	91.4%	12.8%	Unmodified
	38097 (+119)*	38097 (+119)	0.0%	87.2%	Retro-aldol fragment (3)
	38202 (+224)**	38202 (+224)	8.6%	0.0%	Unfragmented (2)

314

¹ See Figure S6 for possible structures of the unassigned fragment.

² The 38163 (+185) Da adduct was observed to shift to a mass of 38146 (+168) Da over the course of 24h, suggesting further fragmentation.

315 **Table S2. Data collection and refinement statistics for the crystal structure of Ldt_{Mt2} reacted with 1.**

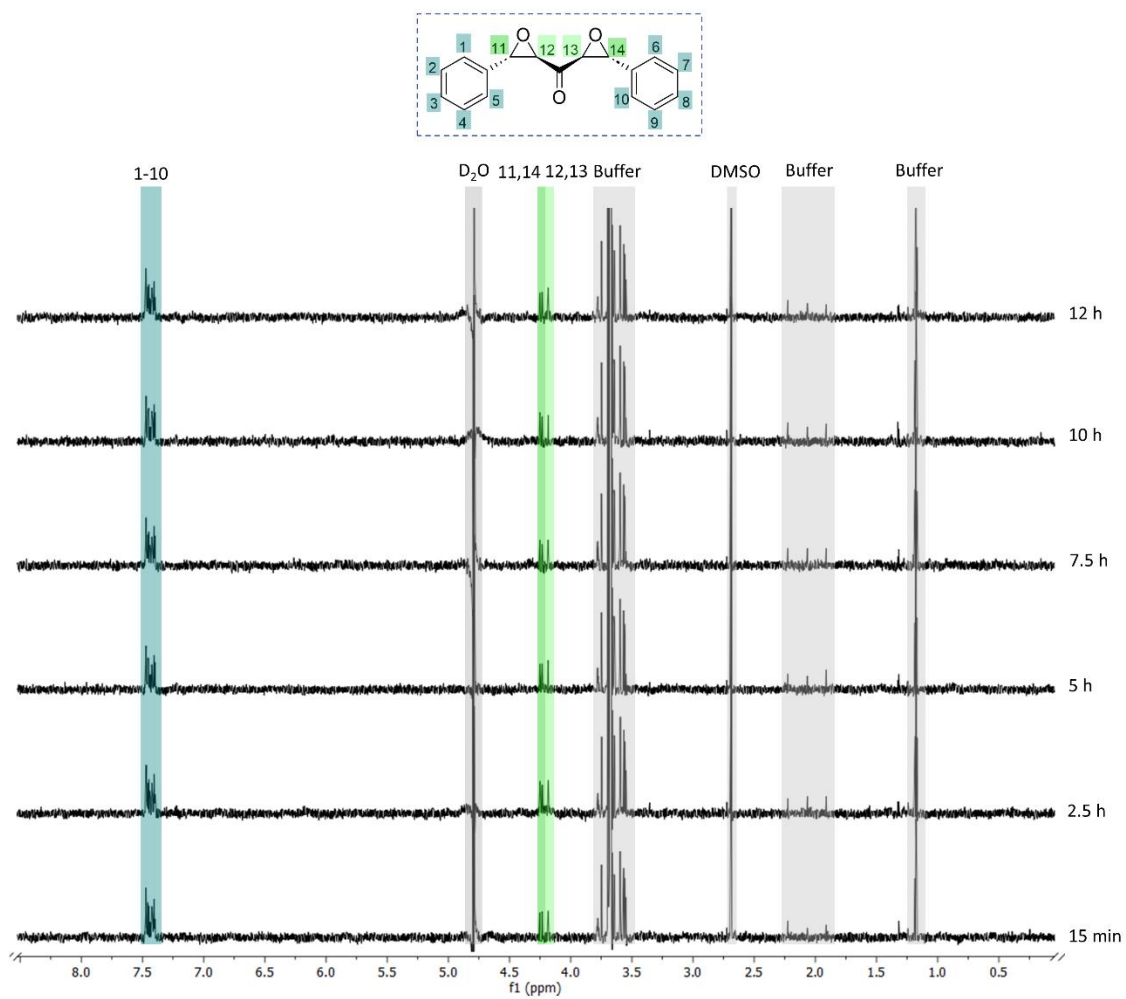
Datasets	Ldt_{Mt2} – 1 (PDB: 8BK3)
Data Collection	
Beamline (Wavelength, Å)	DLS I03 (0.9763)
Detector	Eiger2 XE 16M
Data Processing	Xia2 dials
Space group	<i>P</i> 1 2 ₁ 1
Cell dimensions	
<i>a, b, c</i> (Å)	60.93, 95.06, 75.53
α, β, γ (°)	90.00, 92.60, 90.00
No. of molecules/ASU	2
No. reflections	46835 (4654)*
Resolution (Å)	75.46-2.15 (2.23-2.15)*
<i>R</i> _{merge} (I)	0.167 (1.351)*
<i>I</i> / σ	10.2 (1.1)*
CC-1/2	0.97 (0.7)*
Completeness (%)	100.0 (99.5)*
Multiplicity	7.0 (7.0)*
Wilson B value (Å ²)	28.02
Refinement	
	PHENIX
<i>R</i> _{work} / <i>R</i> _{free}	0.2176/0.2487
No. atoms	6129
- Enzyme	5340
- Ligand	46
- Water	743
Average B-factors	36.62
- Enzyme	36.27
- Ligand	40.92
- Water	38.86
RMS [§] deviations	
- Bond lengths (Å)	0.005
- Bond angles (°)	0.58

316 # ASU = asymmetric unit.

317 § RMS = root mean square.

318 *Highest resolution shell in parentheses.

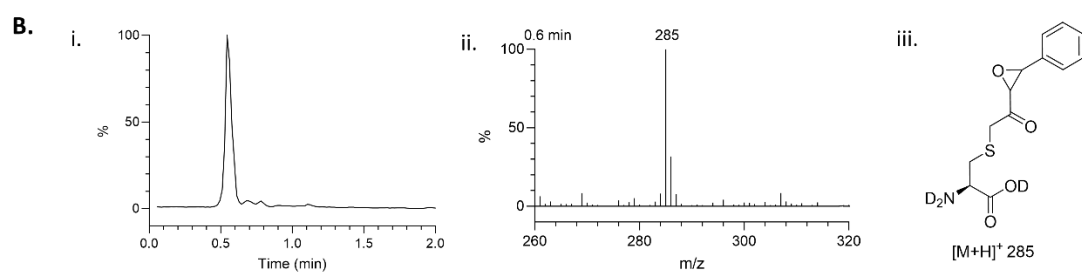
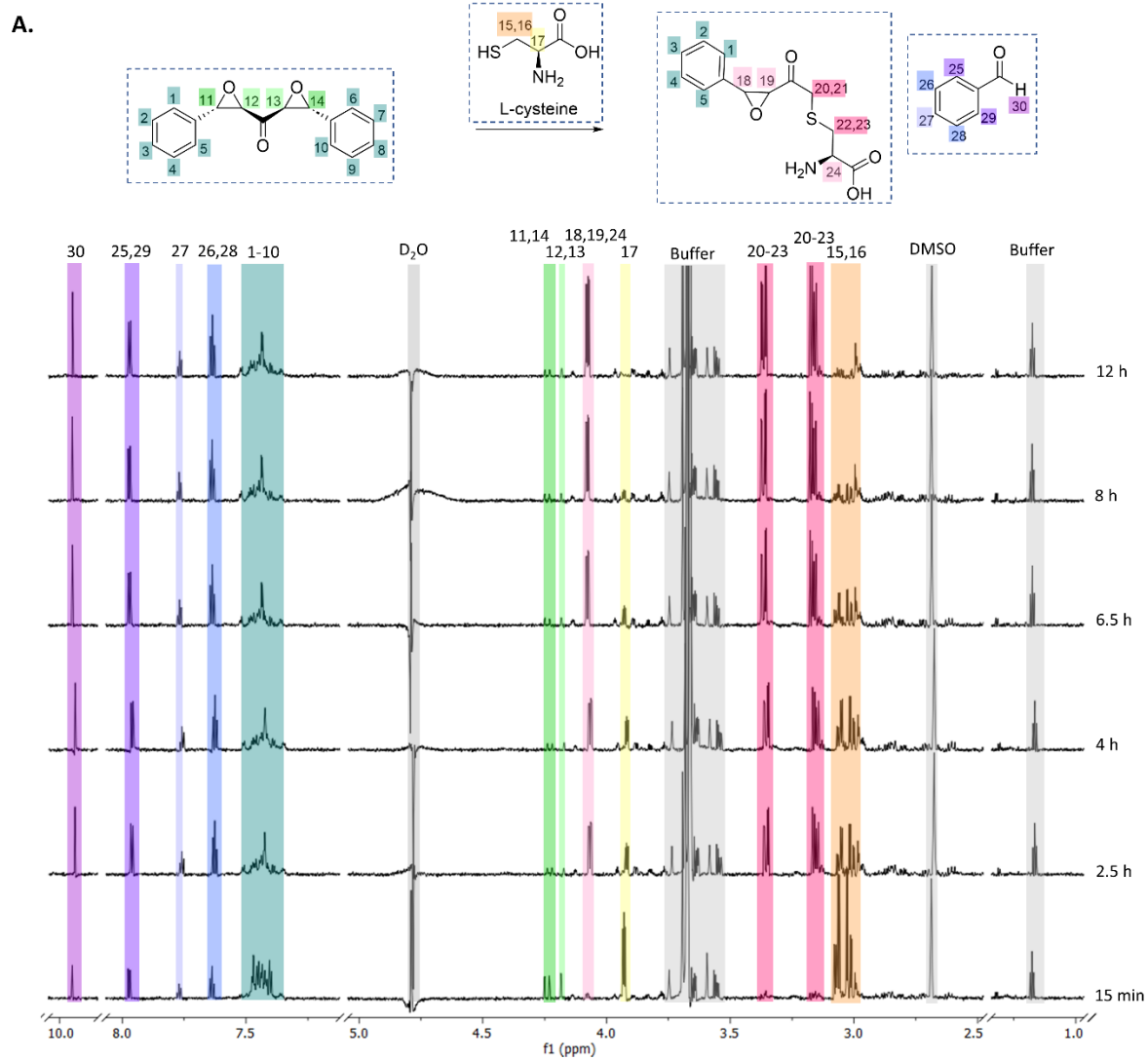
319



320

321 **Figure S3. Stability of DEK 1 in aqueous solution.** A solution of DEK 1 (250 μM) in 50 mM tris-d11, pH 7.5, 10%
 322 D₂O, was analysed by ¹H-NMR (950 MHz) for up to 12 h. No changes in peaks corresponding to **1** (in blue and
 323 green) in spectra were observed. Buffer and solvent peaks are in grey.

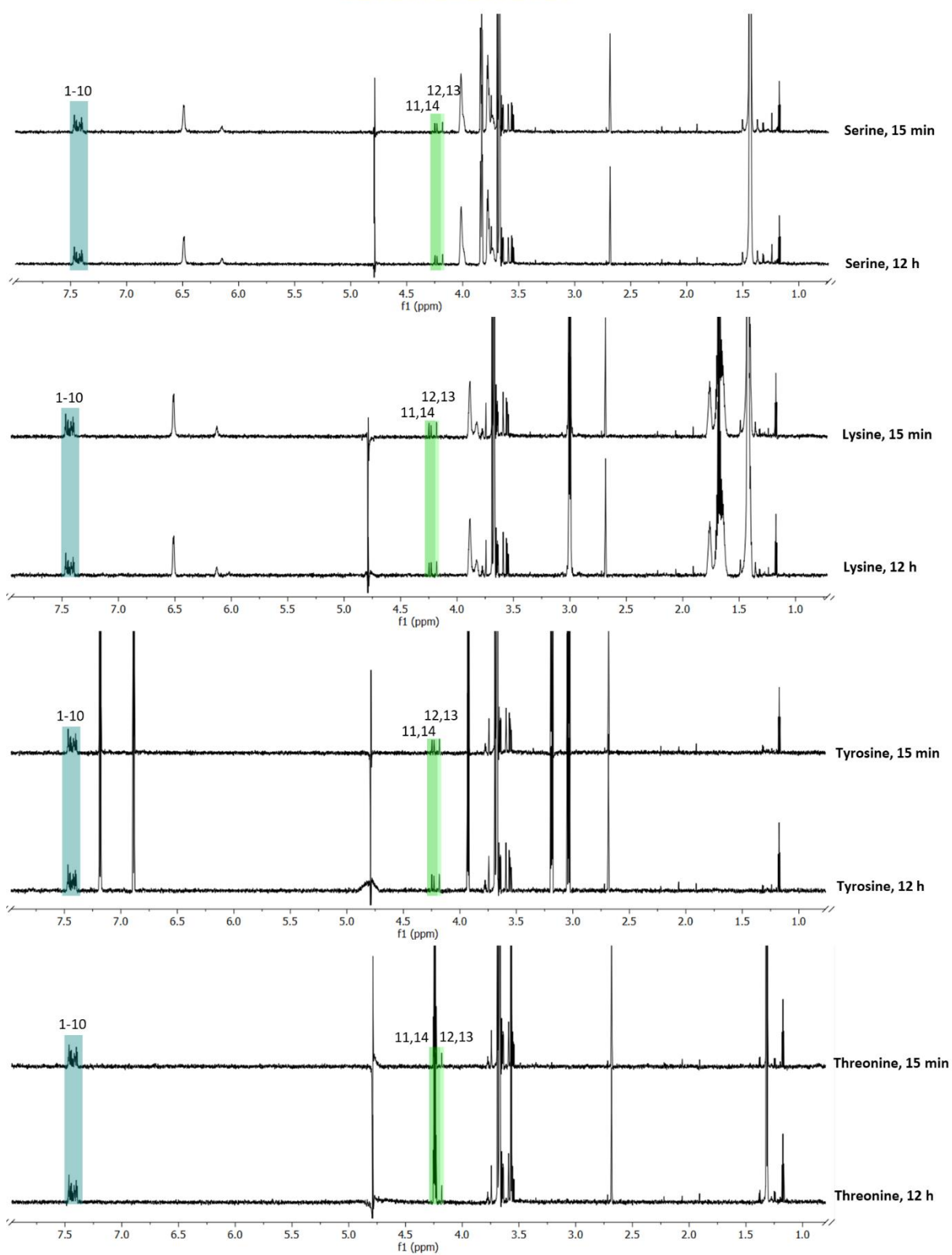
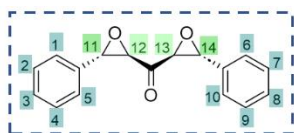
324



325

326 **Figure S4. Reactivity of 1 with L-cysteine.** A solution of 1 (250 μM) was incubated with L-cysteine (250 μM) in 50
 327 mM tris- d_{11} , pH 7.5, 10% D_2O . **A.** The reaction was analysed by $^1\text{H-NMR}$ (950 MHz) for up to 12 h. **B.** The reaction
 328 was analysed by LCMS, 16 h after initiation of the reaction.

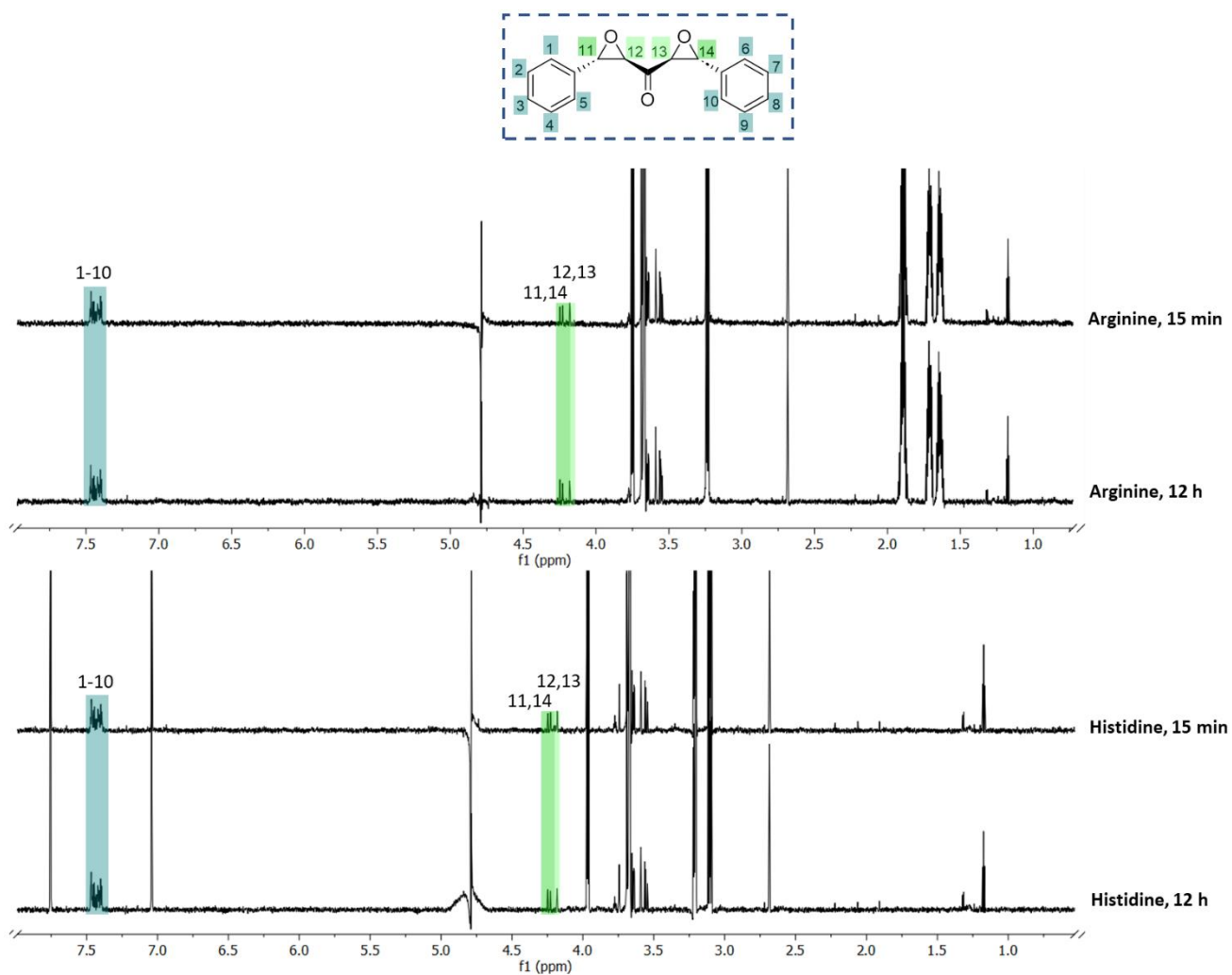
329



330

331 **Figure S5. Reactivity of 1 with serine, lysine, tyrosine, threonine, arginine, and histidine. [Continues]**

332

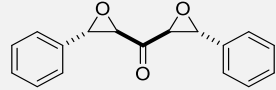
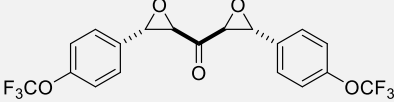
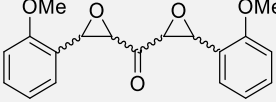
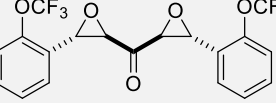
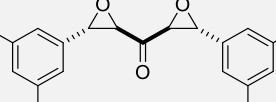
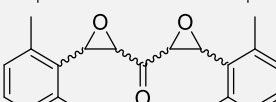
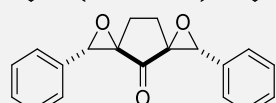
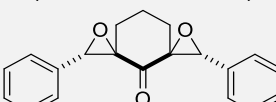
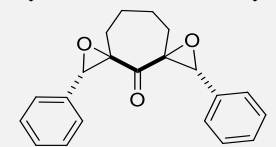
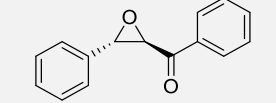


333

334 **Figure S5. Reactivity of 1 with serine, lysine, tyrosine, threonine, arginine, and histidine.** A solution of 1 (250
 335 μM) was incubated with Boc-Ser-OH, Boc-Lys-OH, Tyr, Thr, Arg, or His, (250 μM) in 50 mM Tris- d_{11} , pH 7.5, 10%
 336 D_2O . The reaction was analysed by $^1\text{H-NMR}$ (950 MHz) up to 12 h. DEK 1 apparently did not react with the tested
 337 amino acids under the tested conditions.

338

339 **Table S3. Synthesis and inhibitory characterisation of DEKs 1 and 4-12 with the nucleophilic cysteine enzymes**
 340 **Ldt_{Mt2} and SARS-CoV-2 M^{Pro} and with the nucleophilic serine enzyme BlaC.**

	Structure	Synthetic yield (%)		pIC ₅₀		<i>k</i> _{inact} / <i>K</i> _i (M ⁻¹ s ⁻¹) Ldt _{Mt2}	<i>k</i> _{chem} (M ⁻¹ s ⁻¹)
		Step 1 ^a	Step 2 (dr) ^{a,b}	Ldt _{Mt2}	M ^{Pro}		
1		96	35 (1:0)	6.0 ± 0.03	4.6 ± 0.3	484.3 ± 28.4	<0.8
4		59	11 (1:0)	4.5 ± 0.1	<4.4	<10.0	<0.8
5		78	29 (2:1)	5.1 ± 0.05	<4.4	61.1 ± 2.78	<0.8
6		63	22 (1:0)	5.1 ± 0.06	<4.4	140.6 ± 17.1	<0.8
7		22	16 (1:0)	5.2 ± 0.03	<4.4	80.9 ± 6.74	1.7 ± 0.2
8		7	24 (1.2:1)	4.7 ± 0.04	<4.4	<10.0	1.1 ± 0.2
9		94	52 (1:0)	4.7 ± 0.04	5.9 ± 0.2	25.8 ± 1.41	<0.8
10		58	44 (1:0)	<4.4	<4.4	<10.0	<0.8
11		27	41 (1:0)	<4.4	<4.4	N.D.	N.D.
12		-	-(1:0)	<4.4	<4.4	N.D.	N.D.

341 ^a The 2-step synthesis involved the formation of the diene ketones (Step 1) followed by epoxidation (Step 2), to
 342 yield stereoisomeric mixtures (Figure 1D).

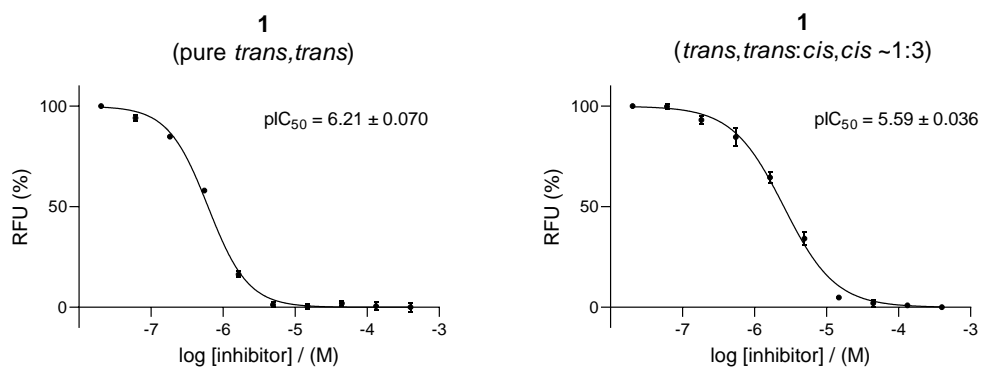
343 ^b Diastereomeric ratio (*trans,trans*:*cis,cis*) following purification, as determined by ¹H NMR analysis.

344

345 **Table S4. Crystal data and structure refinement for 1.**

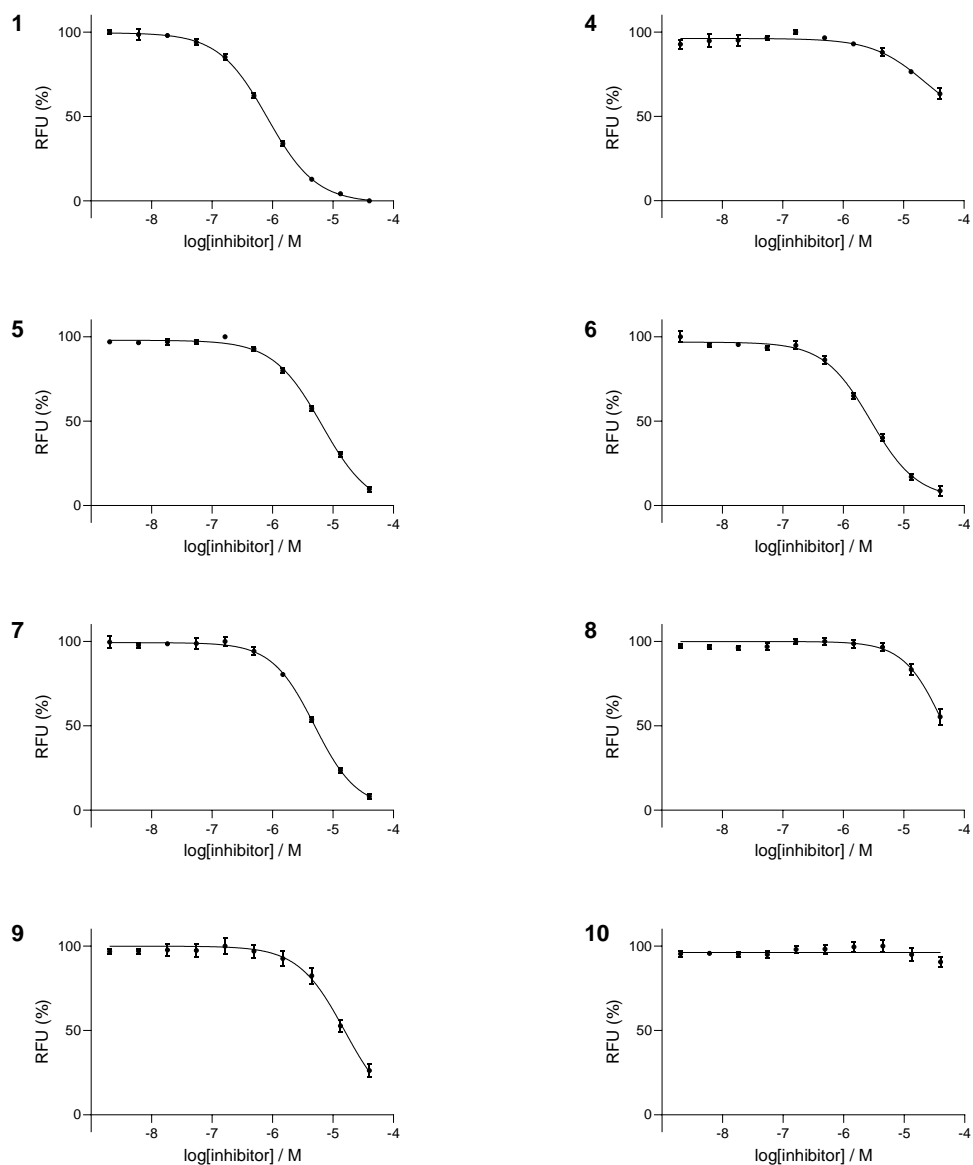
Datasets	1 (CCDC 2262059)	
Empirical formula	C17 H14 O3	
Formula weight	266.30	
Temperature	150 K	
Wavelength	1.54184 Å	
Crystal system	Monoclinic	
Space group	C 2/c	
Cell dimensions	a = 28.7921(3) Å	$\alpha = 90^\circ$
	b = 5.34270(10) Å	$\beta = 92.7637(11)^\circ$
	c = 8.59030(10) Å	$\gamma = 90^\circ$
Volume	1319.89(3) Å ³	
Z	4	
Density (calculated)	1.340 Mg/m ³	
Absorption coefficient	0.742 mm ⁻¹	
F(000)	560	
Crystal size	0.28 x 0.11 x 0.02 mm ³	
Theta range for data collection	3.073 to 75.928°	
Index ranges	-36<=h<=36, -6<=k<=6, -10<=l<=10	
Reflections collected	16701	
Independent reflections	1381 [R(int) = 0.024]	
Completeness to theta = 75.928°	99.9 %	
Absorption correction	Semi-empirical from equivalents	
Max. and min. transmission	0.99 and 0.71	
Refinement method	Full-matrix least-squares on F ²	
Data / restraints / parameters	1381 / 0 / 93	
Goodness-of-fit on F ²	0.9994	
Final R indices [I>2sigma(I)]	R1 = 0.0294, wR2 = 0.0777	
R indices (all data)	R1 = 0.0303, wR2 = 0.0786	
Extinction coefficient	12(2)	
Largest diff. peak and hole	0.25 and -0.13 e.Å ⁻³	

346



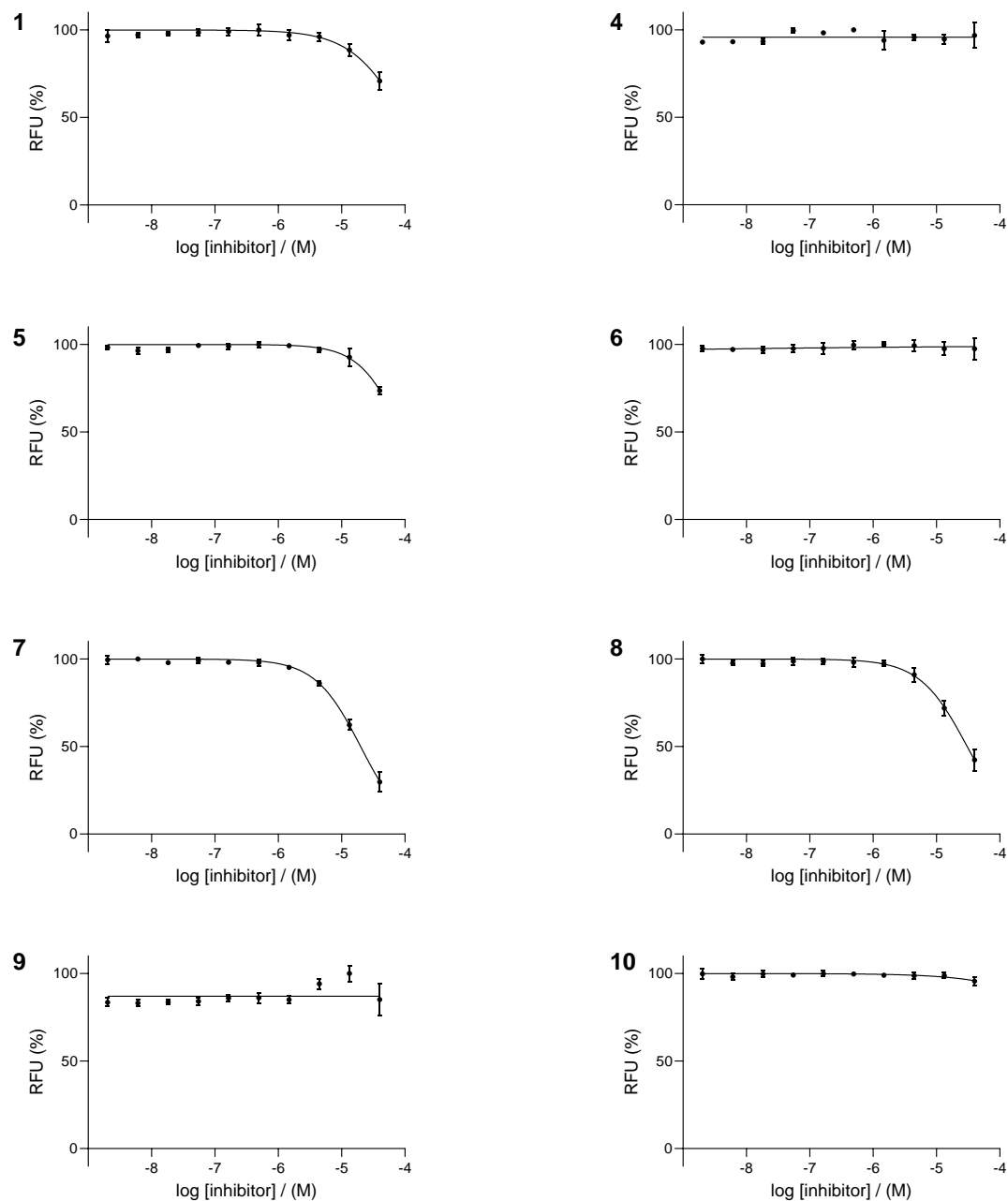
347

348 **Figure S6. Dose-response curves for the pure *trans,trans* isomer of 1 and an isomeric mixture of 1**
 349 **(*trans,trans*:*cis,cis* of ~1:3).** Inhibition assays were carried out using 100 nM Ldt_{Mt2} and 25 μM Probe 1 with 15
 350 min pre-incubation at rt in 50 mM HEPES, pH 7.2 with 0.01% (v/v) Triton X-100. Error bars represent the standard
 351 deviation (n=4). Note that pIC₅₀ values are similar, but imply that the pure *trans,trans* isomer of 1 is the most
 352 active stereoisomer.



353

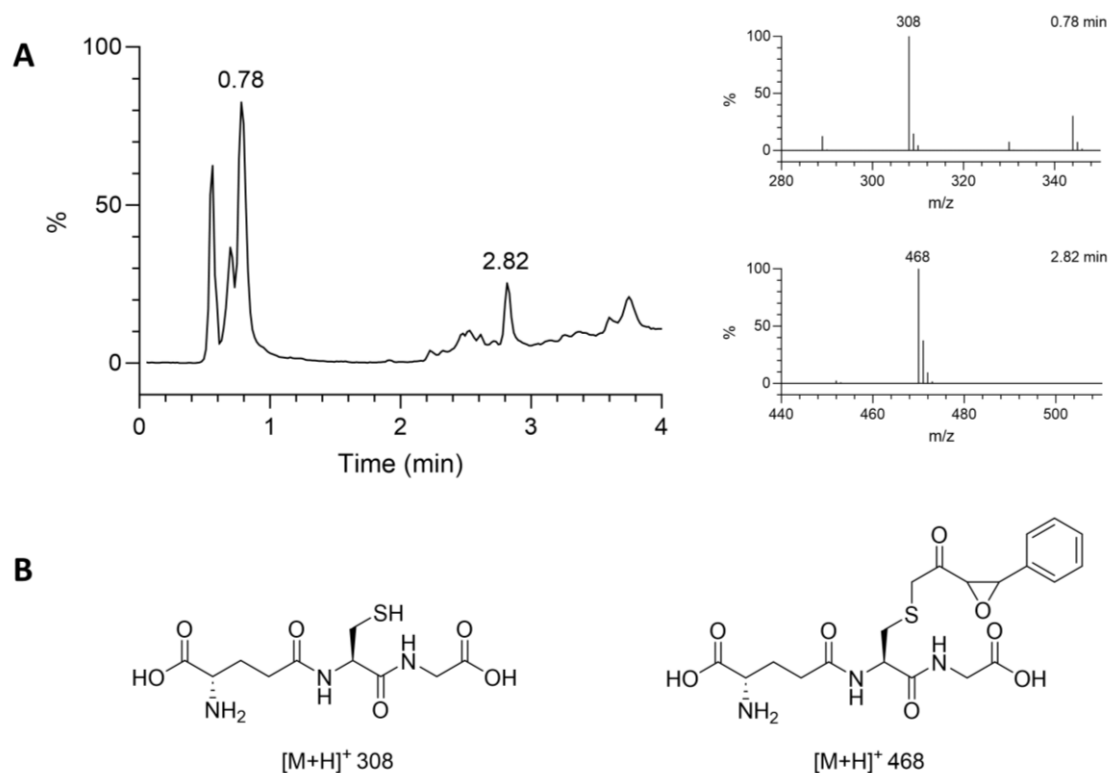
354 **Figure S7. Determination of the second-order rate constant for irreversible inhibition (k_{inact}/K_i) of Ldt_{Mt2} by**
 355 **DEKs 1 and 4-10.** Inhibition assays were carried out using 100 nM Ldt_{Mt2} and 10 μ M Probe 1 with 3 h incubation
 356 at rt in 50 mM HEPES, pH 7.2 with 0.01% (v/v) Triton X-100. Error bars represent the standard deviation (n=4).
 357 Average $(k_{inact}/K_i)_{inhibitor}$ values and compound structures are given in Table S3.



358

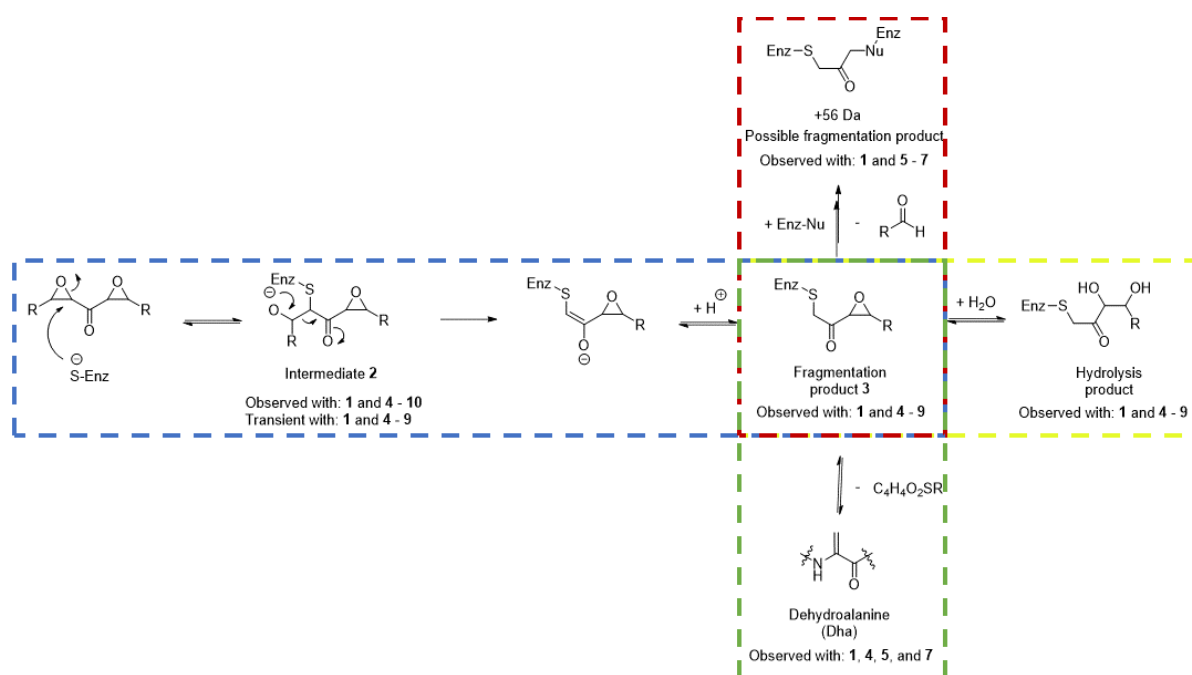
359 **Figure S8. Determination of the intrinsic thiol reactivity rate constant (k_{chem}) for DEKs 1 and 4-10.** Assays were
 360 carried out using 500 nM *L*-glutathione and 10 μM Probe 1 with 16 h incubation at room temperature in 50 mM
 361 HEPES, pH 7.2 with 0.01% (v/v) Triton X-100. Error bars represent the standard deviation ($n=4$). Average k_{chem}
 362 values and compound structures are given in Table S3.

363



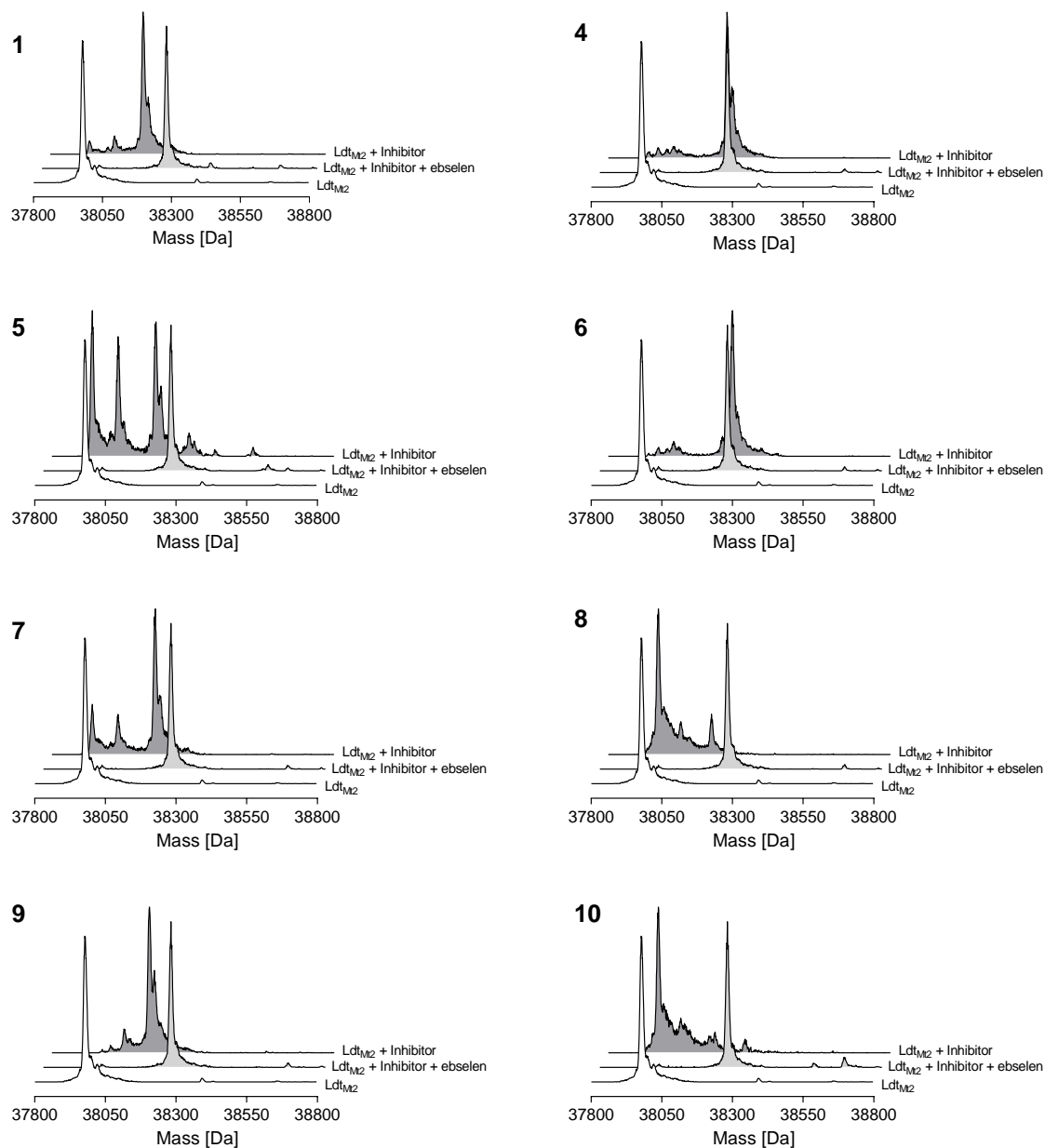
364

365 **Figure S9. LCMS studies of the reaction between GSH and 1.** A solution of **1** (250 μM) and GSH (250 μM) in
 366 50 mM tris pH 7.5 was incubated for 16 h in the presence of TCEP (250 μM), then analysed by LCMS operating in
 367 the positive ion mode. **B.** The compounds eluting at 0.78 min and 2.82 min correspond to unreacted GSH and
 368 GSH reacted with **1** (apparently leading to the fragmented species analogous to **3**), respectively.



369

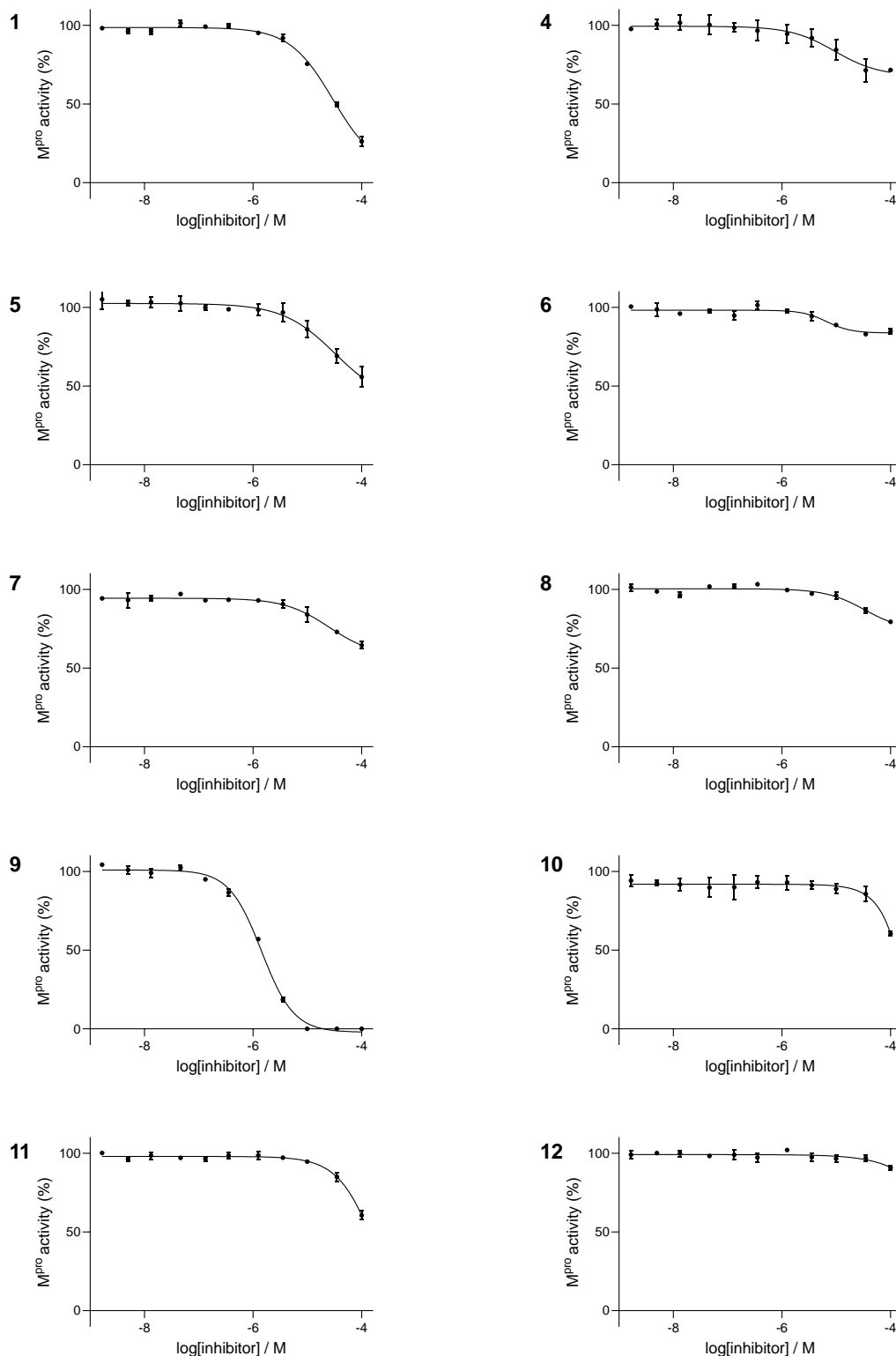
370 **Figure S10. Summary of the reactions of DEKs with nucleophilic cysteine enzymes.** The DEKs are proposed to
 371 inhibit nucleophilic cysteine enzymes via initial reaction of the nucleophilic cysteine with one of the epoxides,
 372 followed by retro-aldol reaction (blue outline). Initial reaction at the DEK carbonyl followed by rearrangement is
 373 also possible (Figure 2C). The fragmentation product **3** (Figure 2) obtained after retro-aldol reaction was
 374 sometimes (as indicated by compound numbers) observed (by MS analysis) to further react to give: (i)
 375 the corresponding hydrolysis product, likely through hydrolytic ring opening of its epoxide (yellow outline), or (ii)
 376 a dehydroalanine (Dha) residue (green outline). Another unassigned product corresponding to a mass shift of +57
 377 Da compared to the unmodified enzyme was (sometimes) observed (red outline). Among other possibilities, the
 378 +57 Da fragmentation product(s) may arise through reaction with another nucleophilic residue in the active site,
 379 leading to a cross-linked adduct.



380

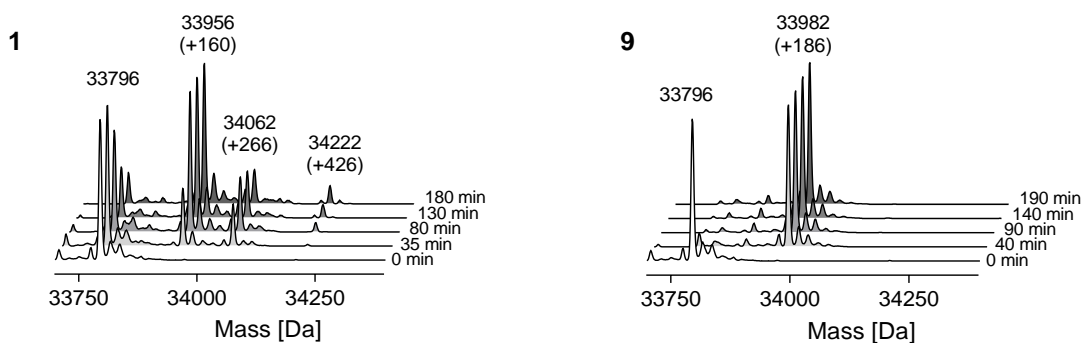
381 **Figure S11. Protein-observed SPE-MS based Cys354 selectivity assays.** Ldt_{Mt2} (1 μM) was preincubated with
 382 ebselen (a reported Ldt_{Mt2} inhibitor⁸ which reacts with the nucleophilic Cys354, 10 μM) for 1 h in 50 mM Tris, pH
 383 7.5. Inhibitors **1** and **4 – 10** (100 μM) were then added and samples were analysed after an additional 24 h
 384 incubation at room temperature using SPE-MS. The spectrum in white corresponds to Ldt_{Mt2} reacted with
 385 ebselen. The spectrum in light grey corresponds to Ldt_{Mt2} reacted with the specified inhibitor, following
 386 preincubation with ebselen. The spectrum in dark grey corresponds to Ldt_{Mt2} reacted with the specified inhibitor.
 387 Deconvoluted spectra, obtained using the maximum entropy algorithm in the MassHunter Workstation
 388 Qualitative Analysis B.07.00 program (Agilent), are shown.

389



390

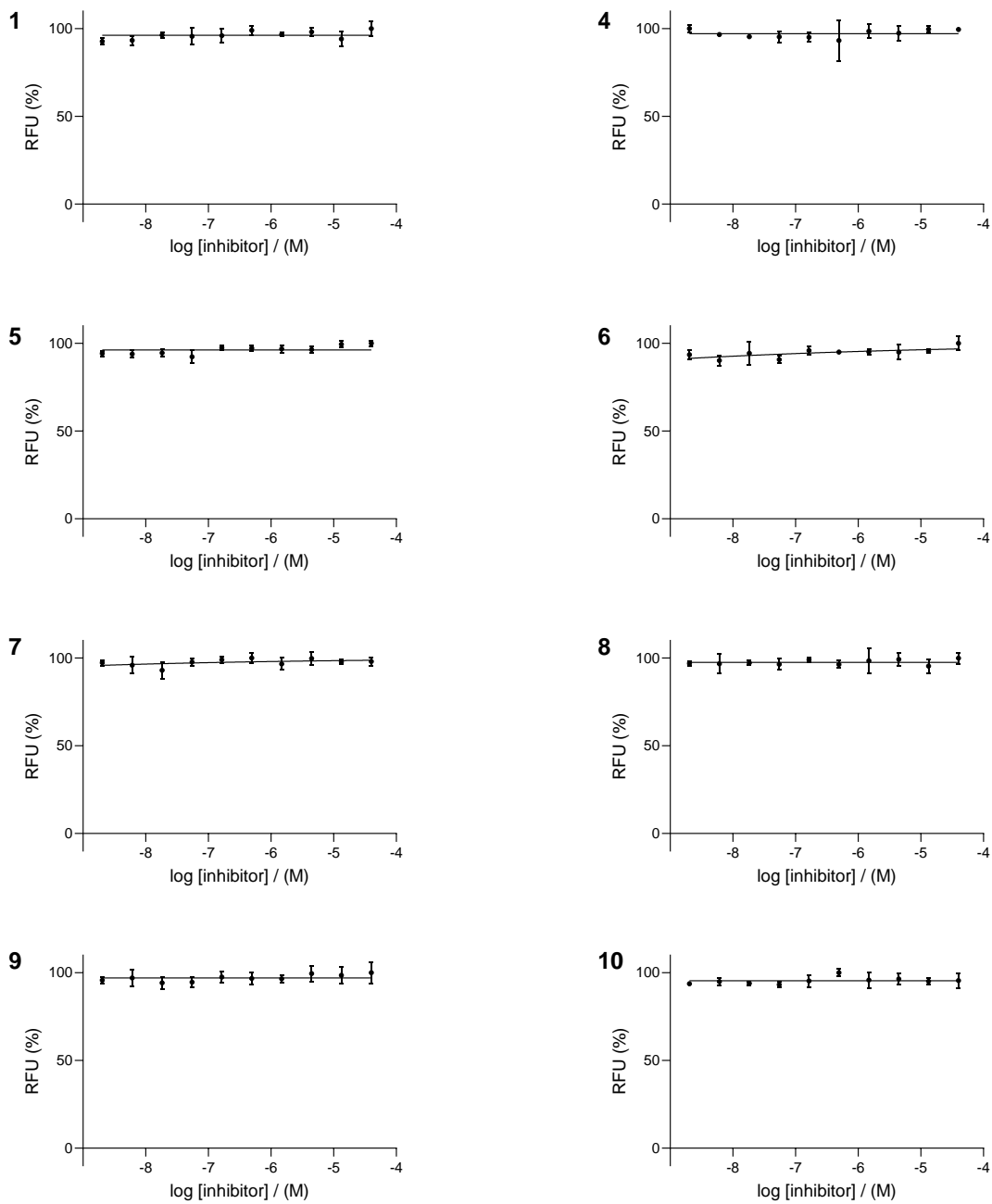
391 **Figure S12. Representative dose-response curves for DEKs 1 and 4-11 and the mono-epoxide ketone 12 with**
 392 **SARS-CoV-2 M^{Pro}.** Inhibition assays were carried out using 150 nM M^{Pro} and 2 μ M 37mer peptide, with 15 min
 393 pre-incubation at rt in 20 mM HEPES, pH 7.5, 50 mM NaCl and M^{Pro} activity was determined by SPE-MS.⁵ Error
 394 bars represent the standard deviation of technical duplicates (n=2). Assays were performed in independent
 395 duplicates, each composed of technical duplicates; average pIC₅₀ values and compound structures are given in
 396 Table S3.



397

398 **Figure S13. Protein observed SPE-MS analysis for the reaction of SARS-CoV-2 M^{pro} with DEKs 1 and 9.** M^{pro} (2
 399 μM) was incubated with DEKs 1 and 9 (20 μM) at rt in 20 mM HEPES, pH 7.5. Samples were analysed after the
 400 indicated times. Deconvoluted spectra, obtained using the maximum entropy algorithm in the MassHunter
 401 Workstation Qualitative Analysis B.07.00 program (Agilent), are shown. Mass shifts and assignments are
 402 analogous to those described in Table S1 for 1 and 9 for reaction with Ldt_{ME2}.

403



404

405 **Figure S14. Dose-response curves for DEKs 1 and 4-10 with BlaC.** Inhibition assays were carried out using 14 nM
 406 BlaC and 10 μ M FC5⁴ with a 10 min pre-incubation at rt in 100 mM sodium phosphate pH 7.5 with 0.01% (v/v)
 407 Triton X-100. Error bars represent the standard deviation (n=4). Average pIC₅₀ values and compound structures
 408 are given in Table S3.

409

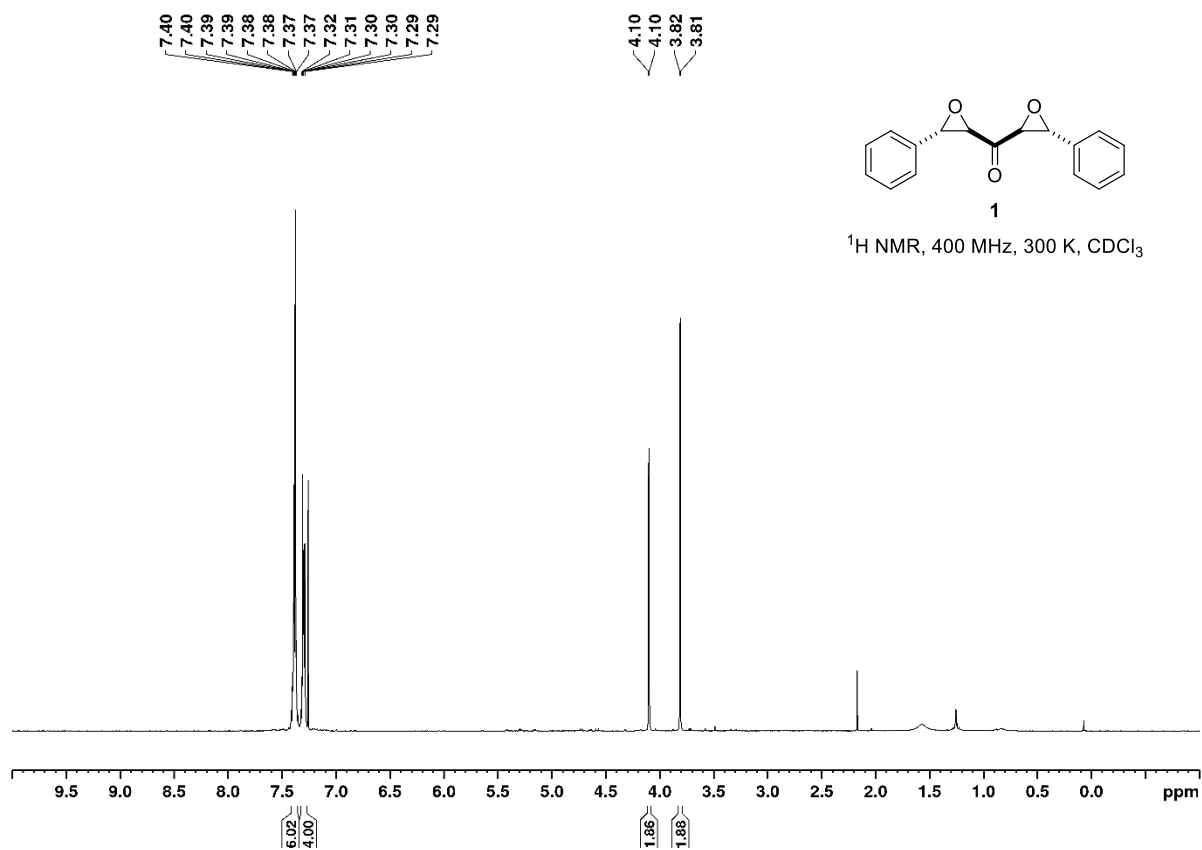
410 **References**

- 411 1. C. T. Lohans, H. T. H. Chan, T. R. Malla, K. Kumar, J. J. A. G. Kamps, D. J. B. McArdle, E. Van
412 Groesen, M. de Munnik, C. L. Tooke, J. Spencer, R. S. Paton, J. Brem and C. J. Schofield,
413 *Angew. Chem. Int. Ed.*, 2019, **58**, 1990-1994.
- 414 2. T. R. Malla, A. Tumber, T. John, L. Brewitz, C. Strain-Damerell, C. D. Owen, P. Lukacik, H. T. H.
415 Chan, P. Maheswaran, E. Salah, F. Duarte, H. Yang, Z. Rao, M. A. Walsh and C. J. Schofield,
416 *Chem. Commun.*, 2021, **57**, 1430-1433.
- 417 3. M. de Munnik, C. T. Lohans, G. W. Langley, C. Bon, J. Brem and C. J. Schofield, *ChemBioChem*,
418 2020, **21**, 368-372.
- 419 4. S. S. Van Berkel, J. Brem, A. M. Rydzik, R. Salimraj, R. Cain, A. Verma, R. J. Owens, C. W. G.
420 Fishwick, J. Spencer and C. J. Schofield, *J. Med. Chem.*, 2013, **56**, 6945-6953.
- 421 5. T. R. Malla, L. Brewitz, D.-G. Muntean, H. Aslam, C. D. Owen, E. Salah, A. Tumber, P. Lukacik,
422 C. Strain-Damerell, H. Mikolajek, M. A. Walsh and C. J. Schofield, *J. Med. Chem.*, 2022, **65**,
423 7682-7696.
- 424 6. M. de Munnik, P. A. Lang, F. De Dios Antos, M. Cacho, R. H. Bates, J. Brem, B. Rodríguez-
425 Miquel and C. J. Schofield, *Chem. Sci.*, 2023, **14**, 7262-7278.
- 426 7. A. J. McCoy, R. W. Grosse-Kunstleve, P. D. Adams, M. D. Winn, L. C. Storoni and R. J. Read, *J.*
427 *Appl. Crystallogr.*, 2007, **40**, 658-674.
- 428 8. M. de Munnik, C. T. Lohans, P. A. Lang, G. W. Langley, T. R. Malla, A. Tumber, C. J. Schofield
429 and J. Brem, *Chem. Commun.*, 2019, **55**, 10214-10217.
- 430 9. P. D. Adams, P. V. Afonine, G. Bunkóczi, V. B. Chen, I. W. Davis, N. Echols, J. J. Headd, L.-W.
431 Hung, G. J. Kapral, R. W. Grosse-Kunstleve, A. J. McCoy, N. W. Moriarty, R. Oeffner, R. J. Read,
432 D. C. Richardson, J. S. Richardson, T. C. Terwilliger and P. H. Zwart, *Acta Crystallogr. D*, 2010,
433 **66**, 213-221.
- 434 10. P. Emsley, B. Lohkamp, W. G. Scott and K. Cowtan, *Acta Crystallogr. D*, 2010, **66**, 486-501.
- 435 11. D. Liebschner, P. V. Afonine, N. W. Moriarty, B. K. Poon, O. V. Sobolev, T. C. Terwilliger and P.
436 D. Adams, *Acta Crystallogr. D*, 2017, **73**, 148-157.
- 437 12. L. Palatinus and G. Chapuis, *J. Appl. Crystallogr.*, 2007, **40**, 786-790.
- 438 13. P. Parois, R. I. Cooper and A. L. Thompson, *Chem. Cent. J.*, 2015, **9**.
- 439 14. R. I. Cooper, A. L. Thompson and D. J. Watkin, *J. Appl. Crystallogr.*, 2010, **43**, 1100-1107.
- 440 15. D. G. Gibson, L. Young, R.-Y. Chuang, J. C. Venter, C. A. Hutchison and H. O. Smith, *Nat.*
441 *Methods*, 2009, **6**, 343-345.
- 442 16. A. Arnold, M. Markert and R. Mahrwald, *Synthesis*, 2006, DOI: 10.1055/s-2006-926346, 1099-
443 1102.
- 444 17. W. M. Weber, L. A. Hunsaker, C. N. Roybal, E. V. Bobrovnikova-Marjon, S. F. Abcouwer, R. E.
445 Royer, L. M. Deck and D. L. Vander Jagt, *Bioorg. Med. Chem.*, 2006, **14**, 2450-2461.
- 446 18. V. K. Yadav and K. K. Kapoor, *Tetrahedron*, 1996, **52**, 3659-3668.
- 447 19. US9174960B2, 2015.
- 448 20. K. D. Ashtekar, X. Ding, E. Toma, W. Sheng, H. Gholami, C. Rahn, P. Reed and B. Borhan, *Org.*
449 *Let.*, 2016, **18**, 3976-3979.
- 450 21. E. Aguilera, J. Varela, E. Birriel, E. Serna, S. Torres, G. Yaluff, N. V. De Bilbao, B. Aguirre-López,
451 N. Cabrera, S. Díaz Mazariegos, M. T. De Gómez-Puyou, A. Gómez-Puyou, R. Pérez-Montfort,
452 L. Minini, A. Merlino, H. Cerecetto, M. González and G. Alvarez, *ChemMedChem*, 2016, **11**,
453 1328-1338.
- 454 22. A. Hasaninejad, A. Zare, L. Balooty, H. Mehregan and M. Shekouhy, *Synth. Commun.*, 2010,
455 **40**, 3488-3495.
- 456 23. W. M. Weber, L. A. Hunsaker, S. F. Abcouwer, L. M. Deck and D. L. Vander Jagt, *Bioorg. Med.*
457 *Chem.*, 2005, **13**, 3811-3820.

458

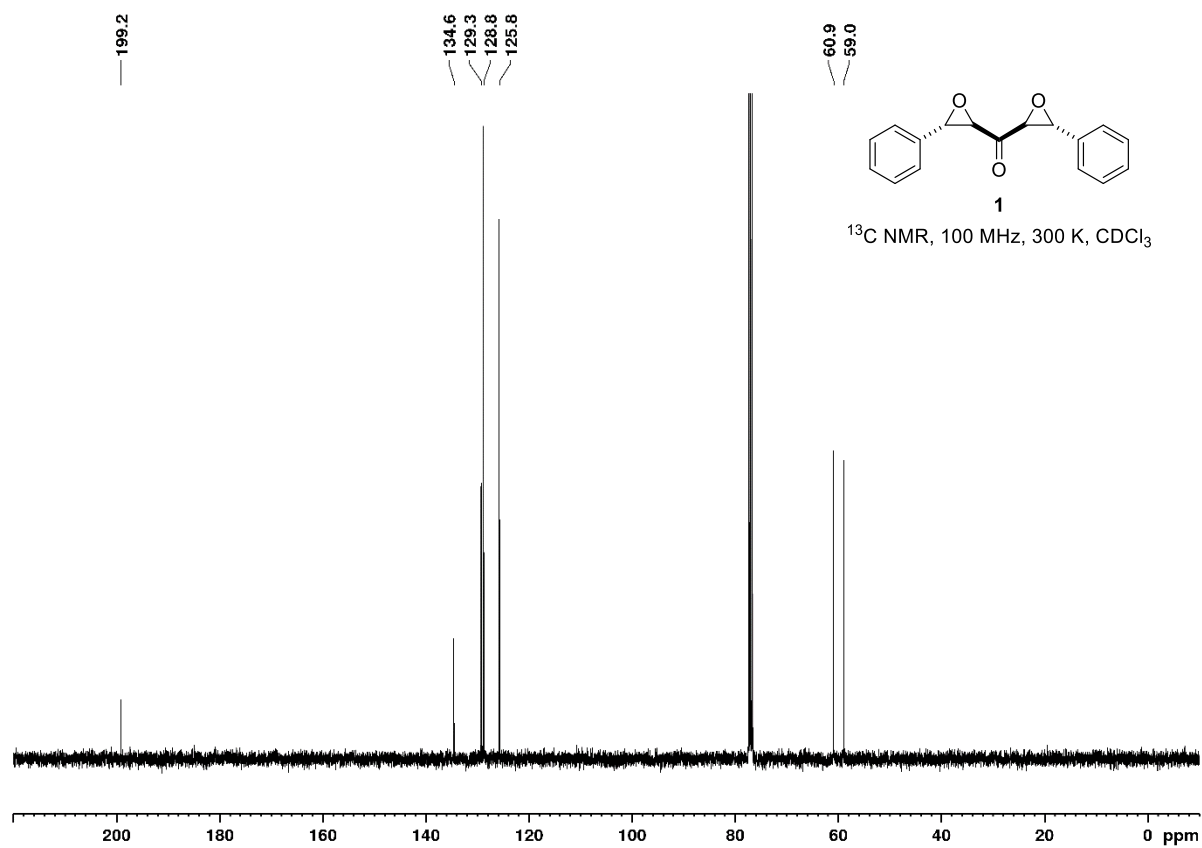
459

460

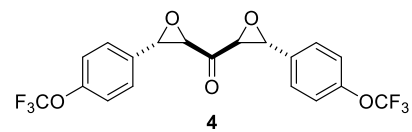
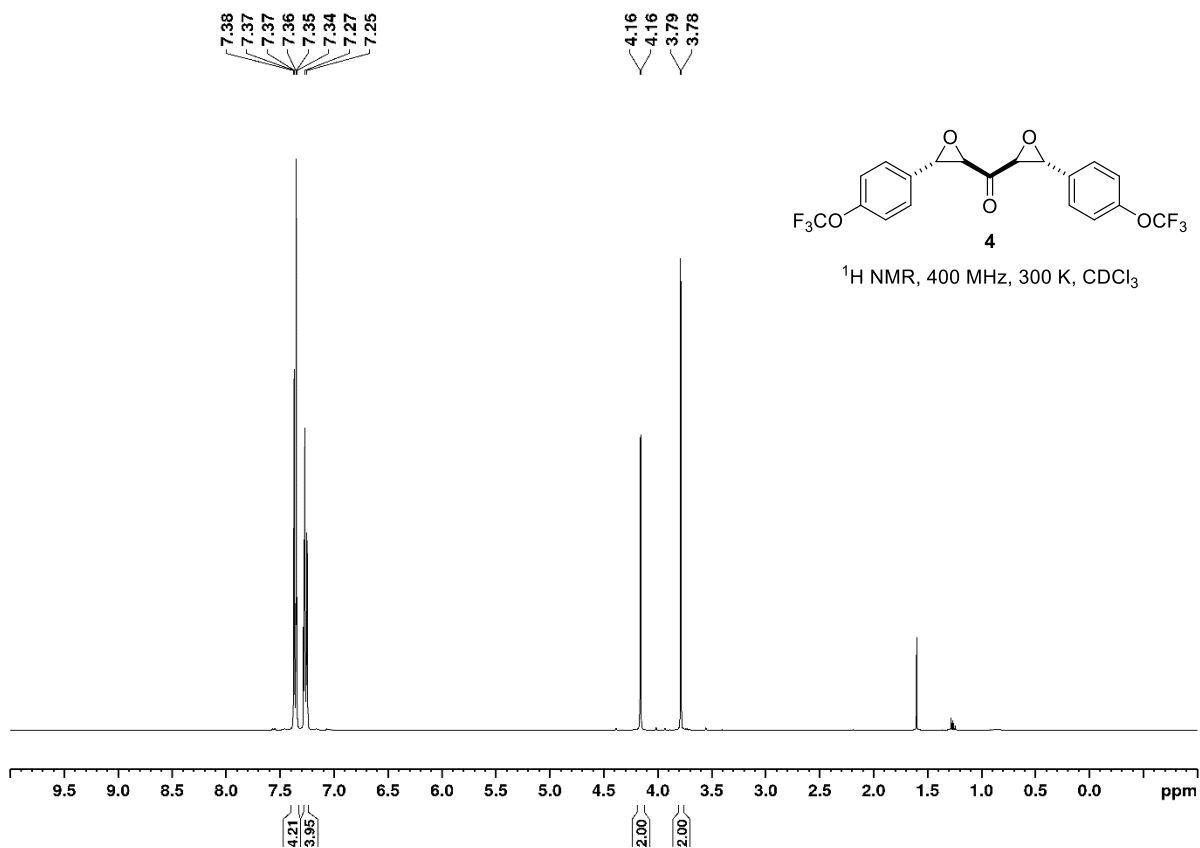


461

462



463

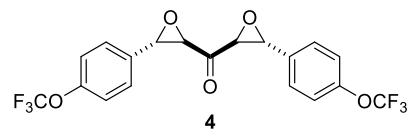
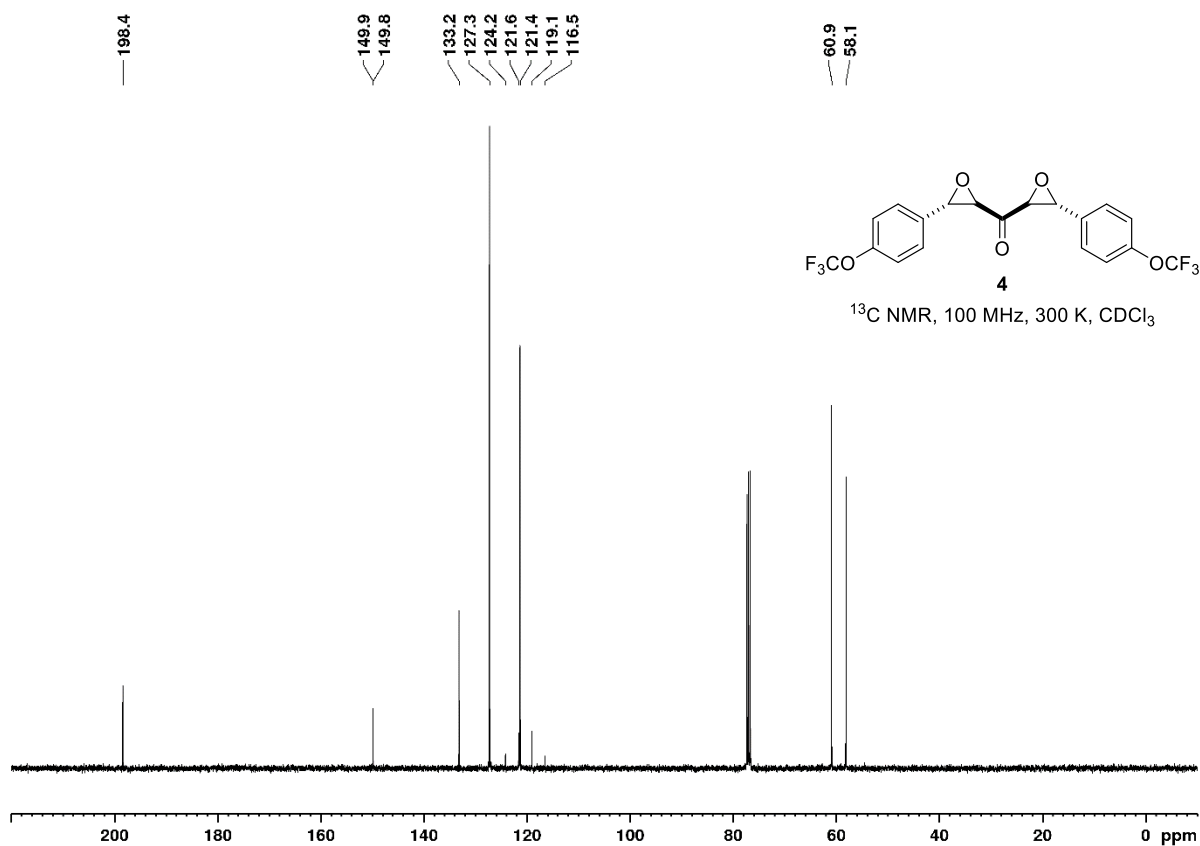


¹H NMR, 400 MHz, 300 K, CDCl₃

464

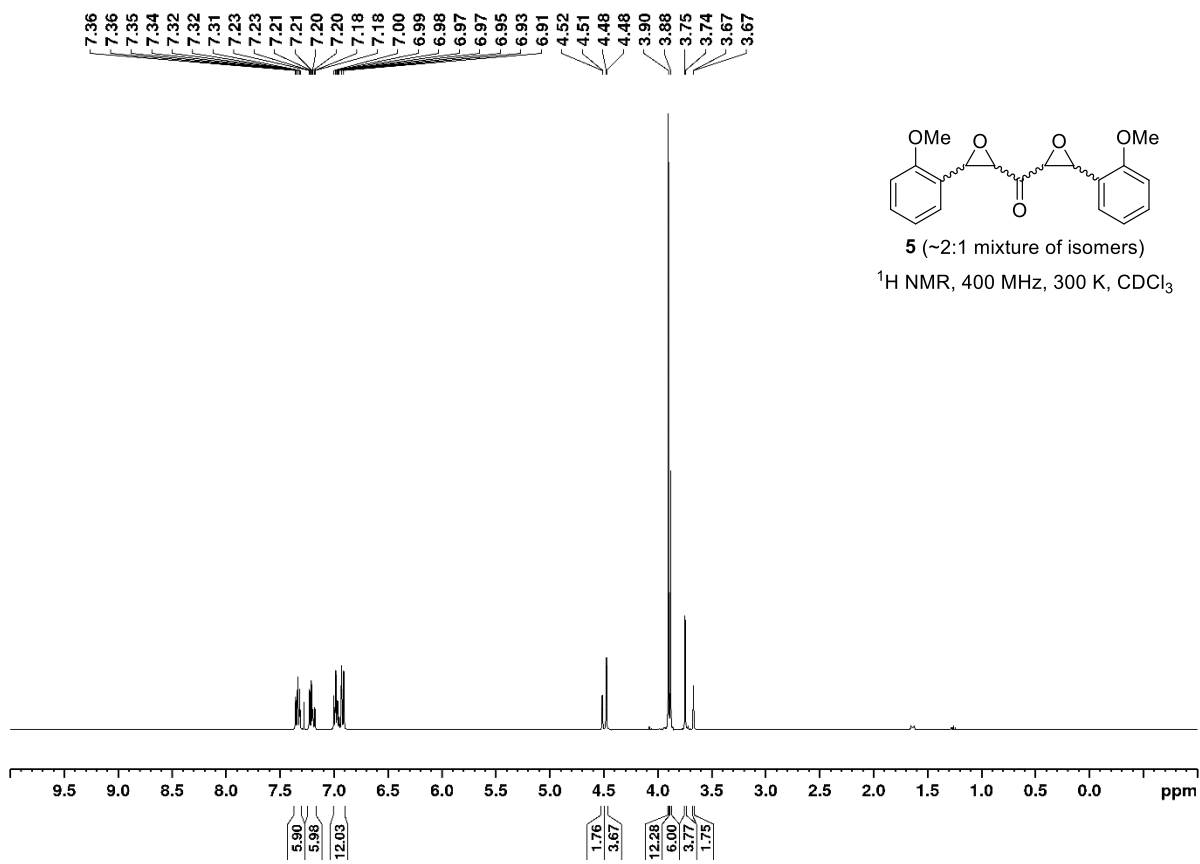
465

466

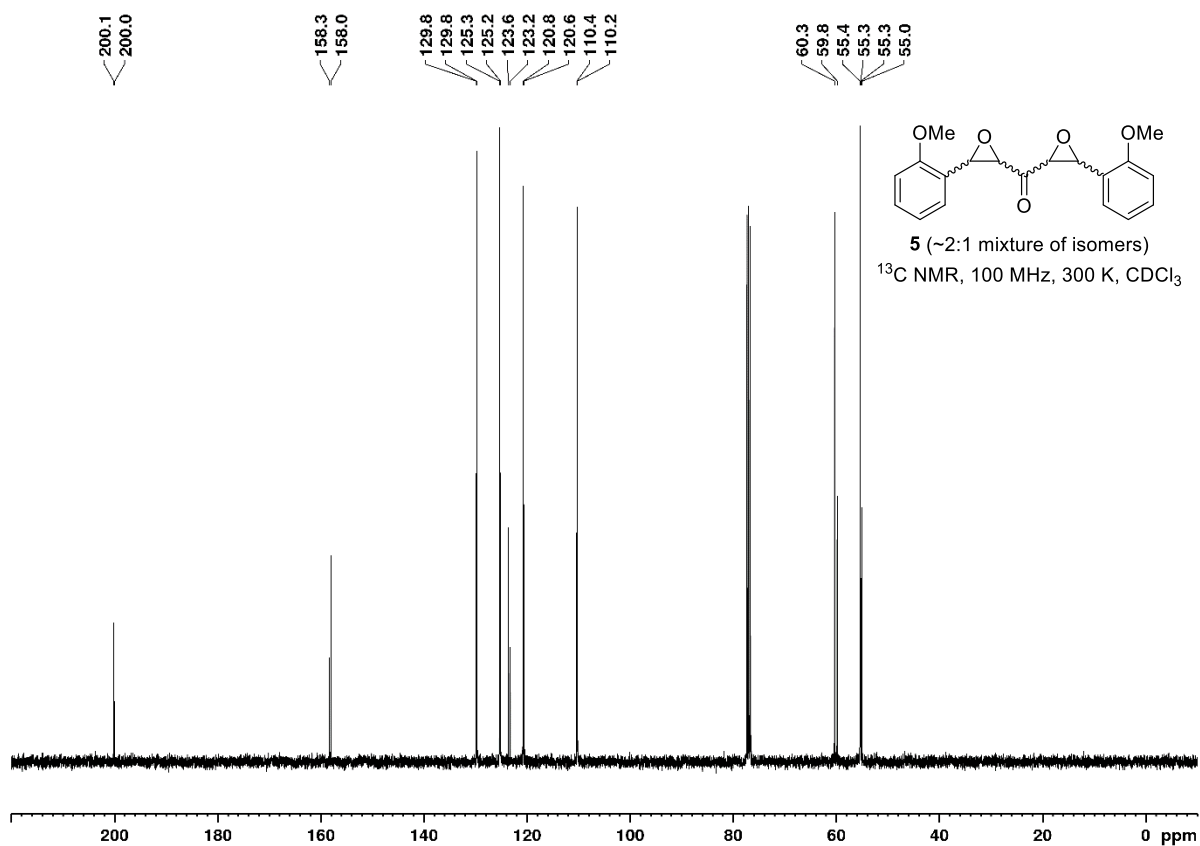


¹³C NMR, 100 MHz, 300 K, CDCl₃

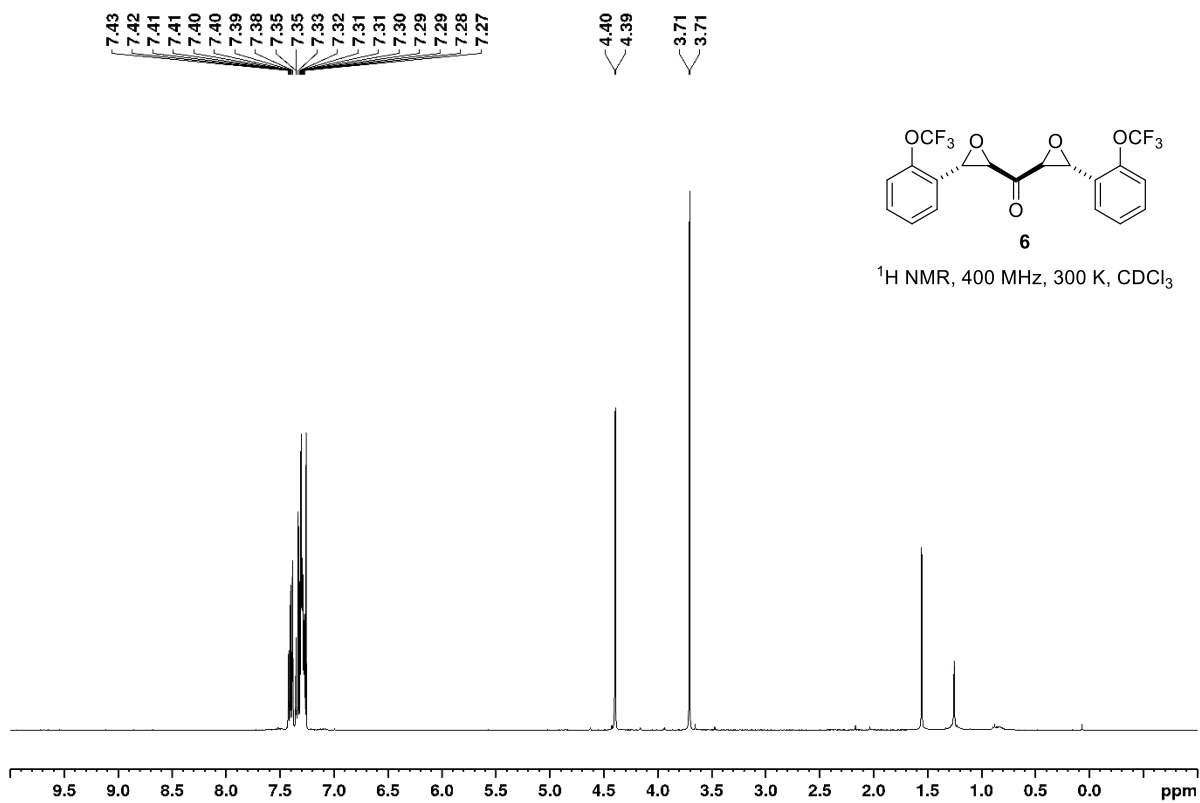
467



468
469
470



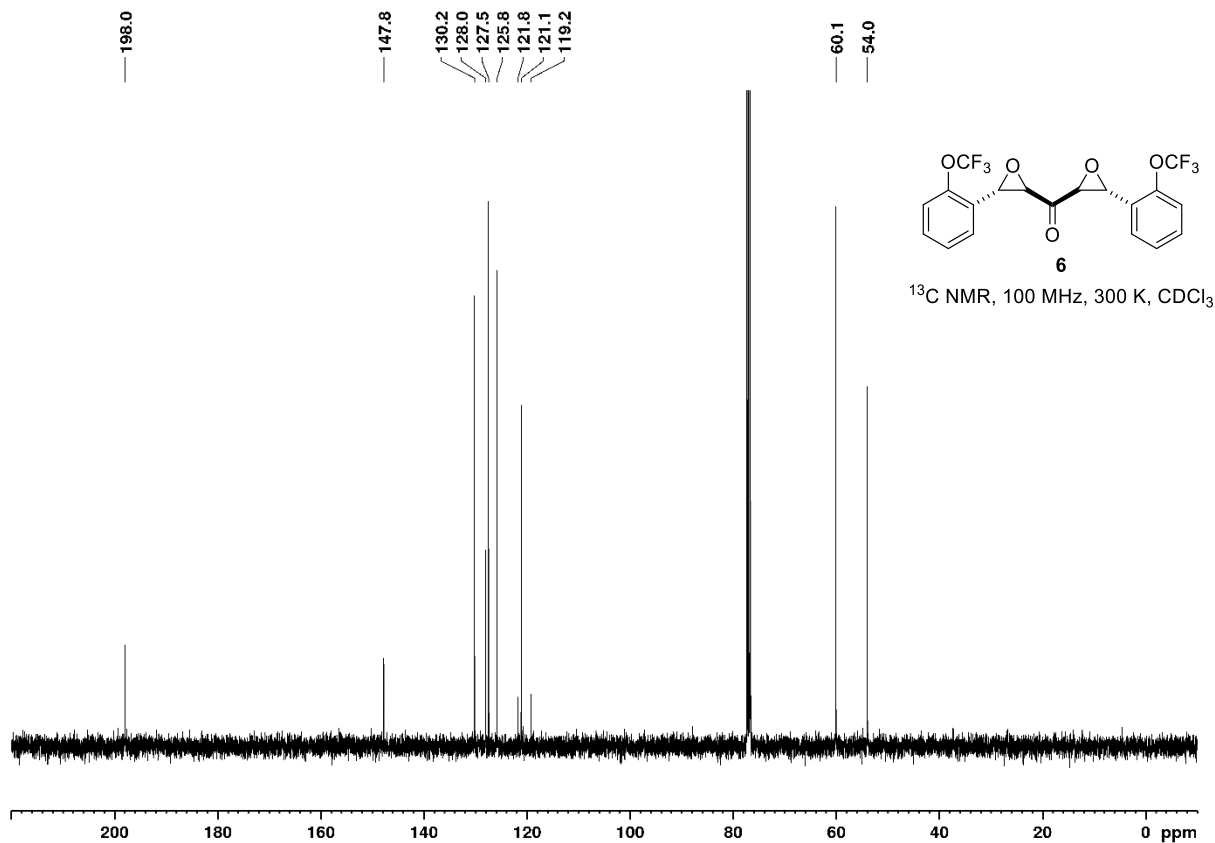
471



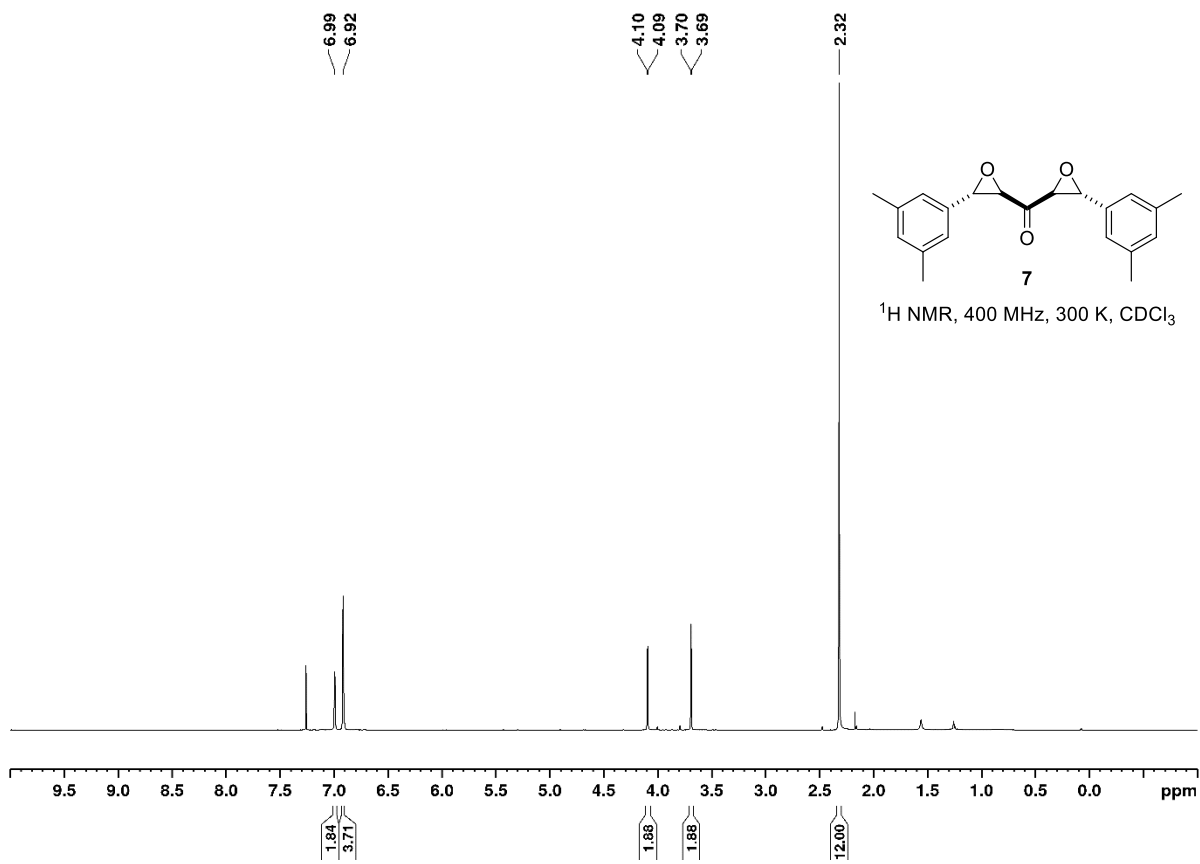
472

473

474



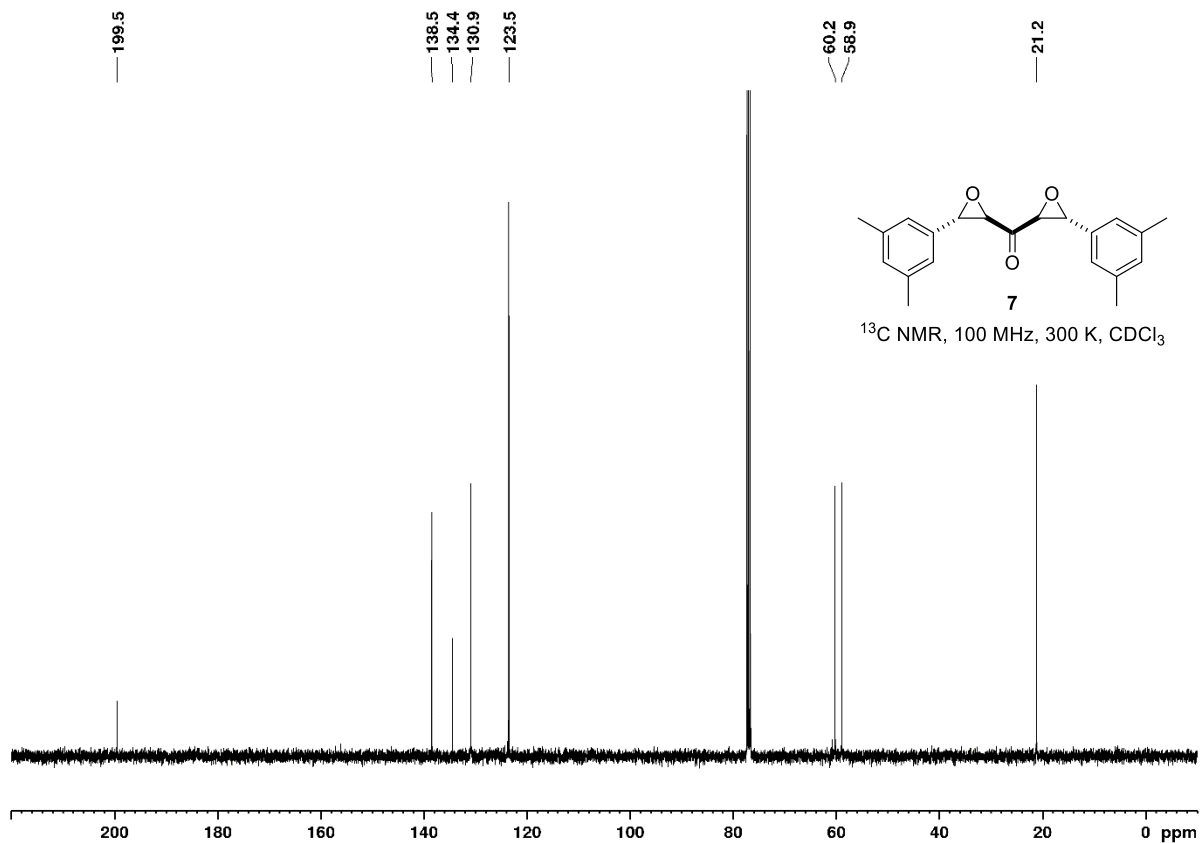
475



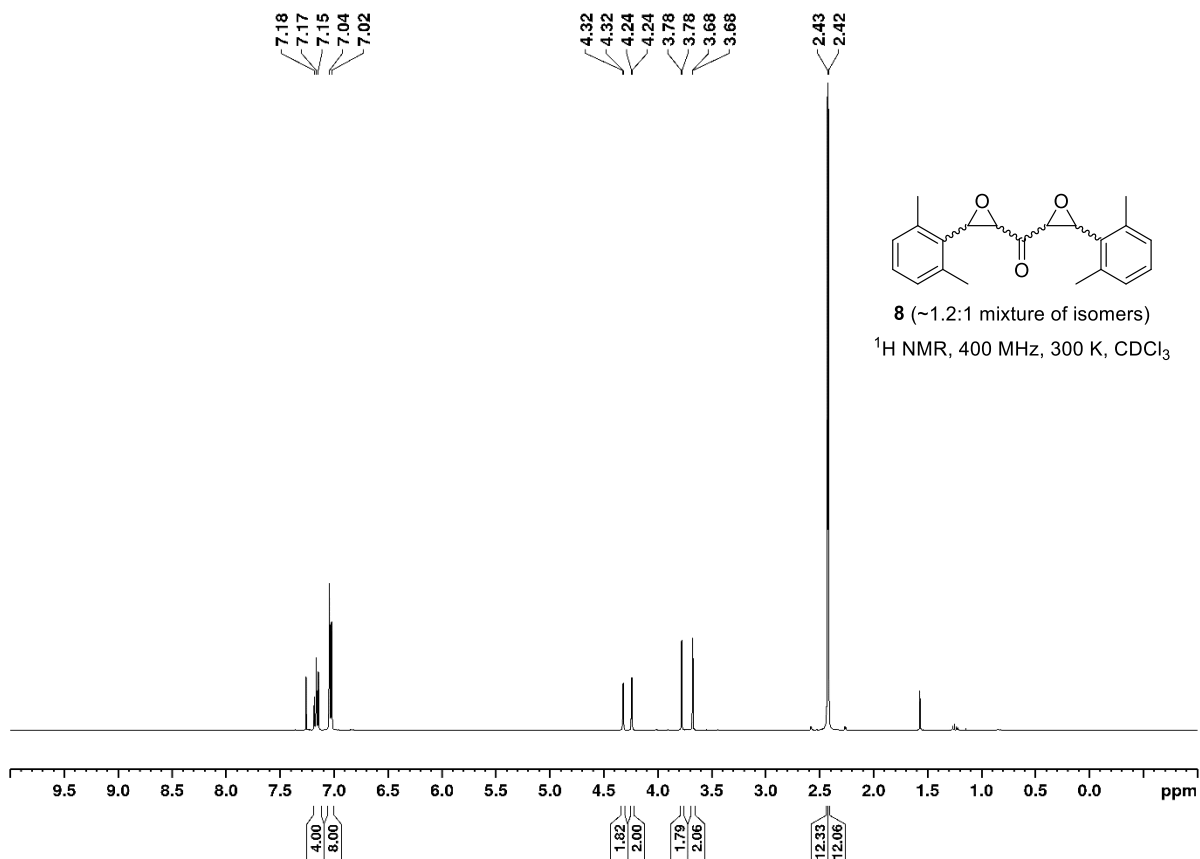
476

477

478



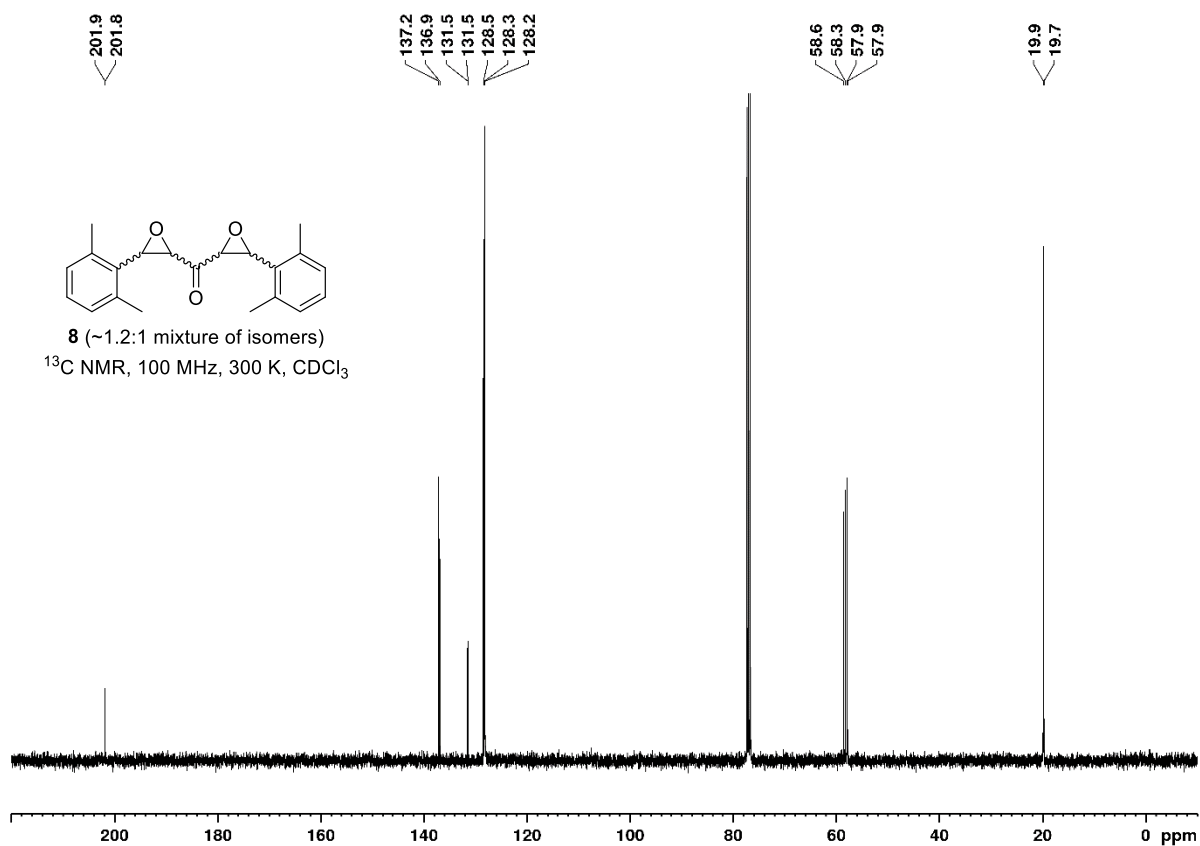
479



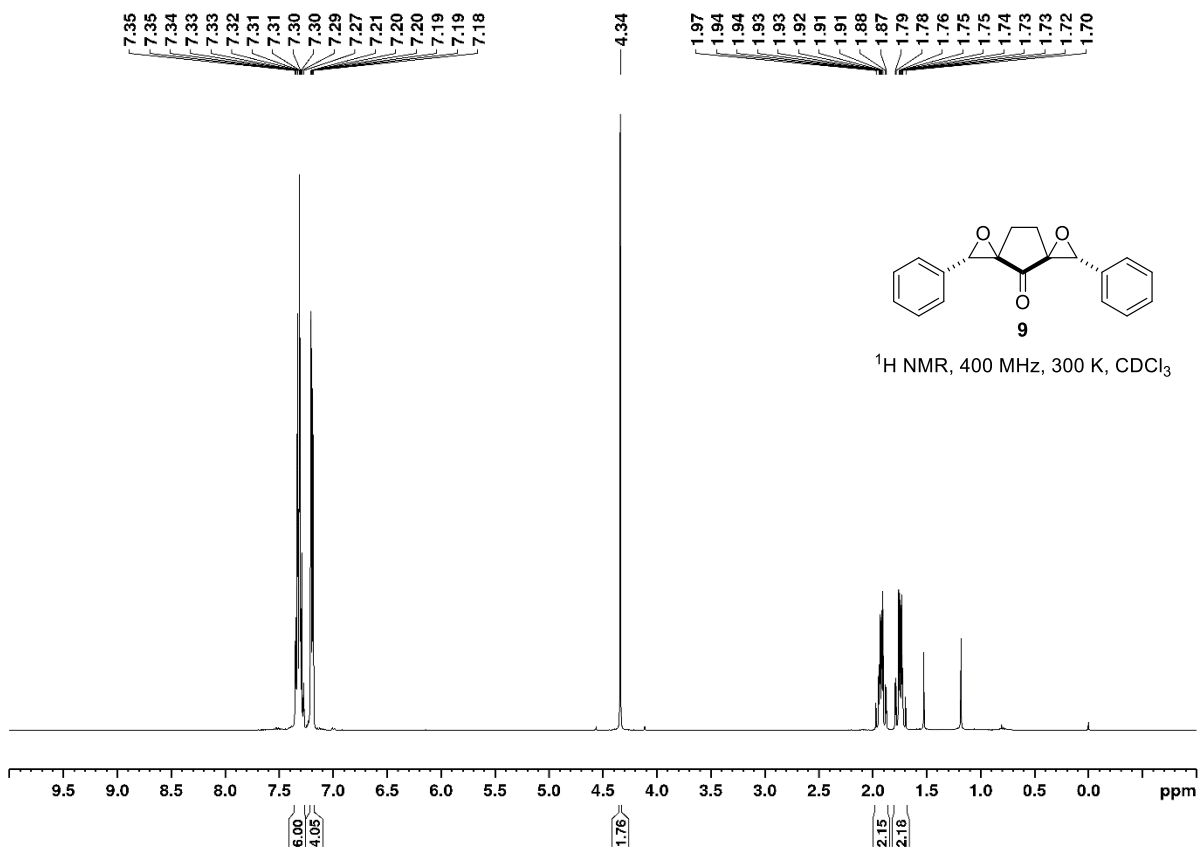
480

481

482



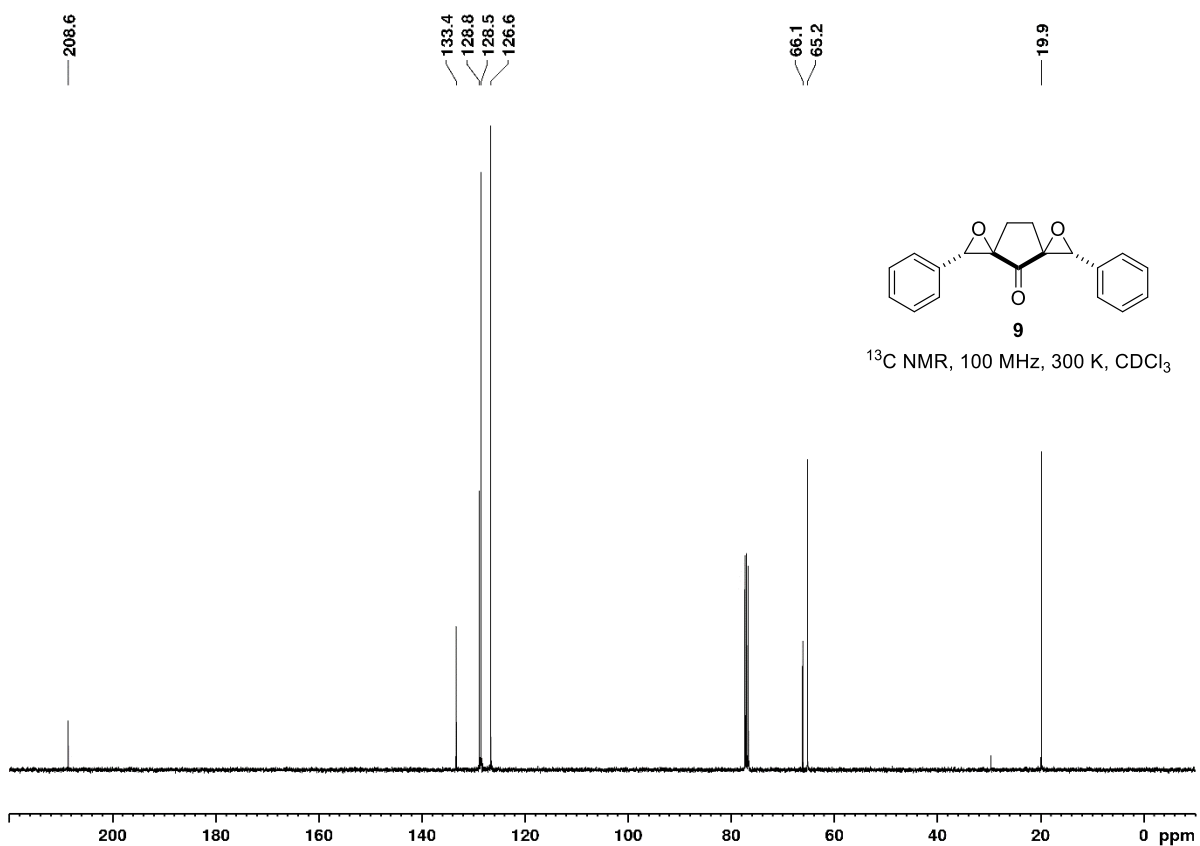
483



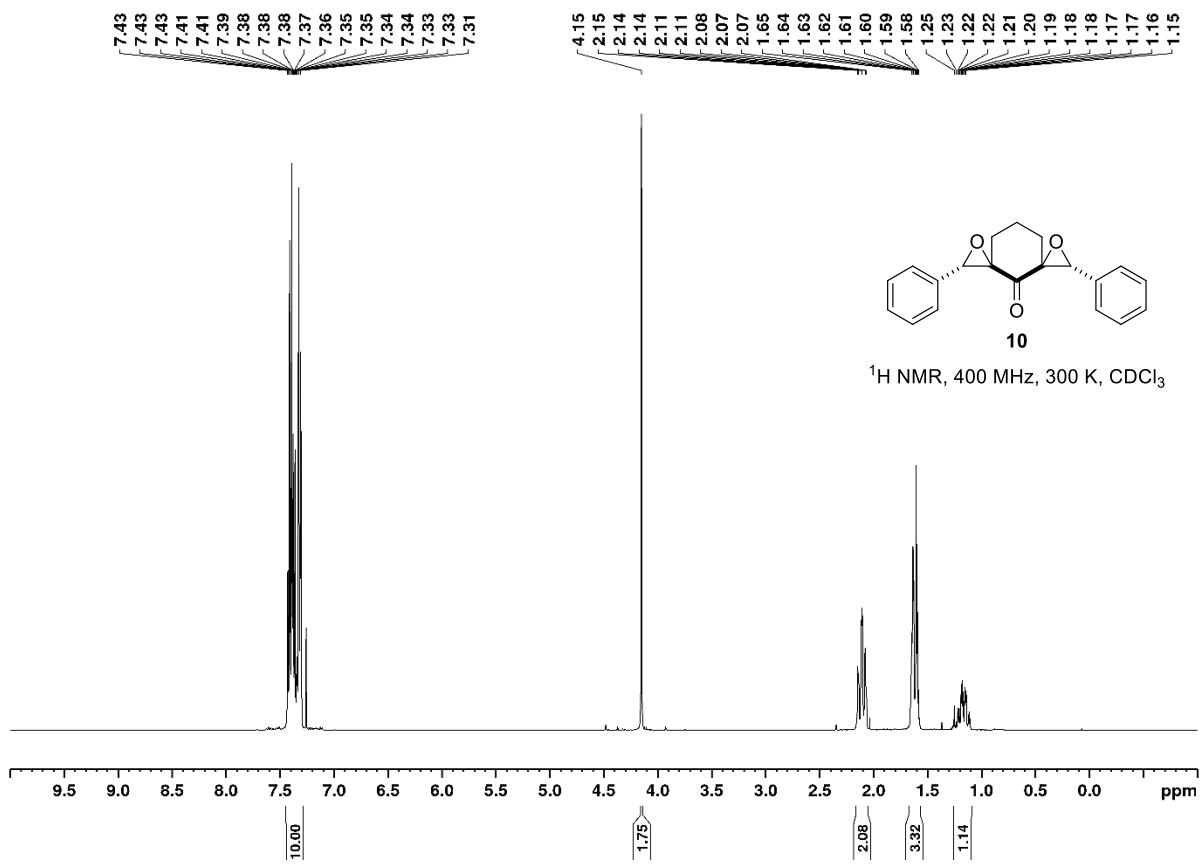
484

485

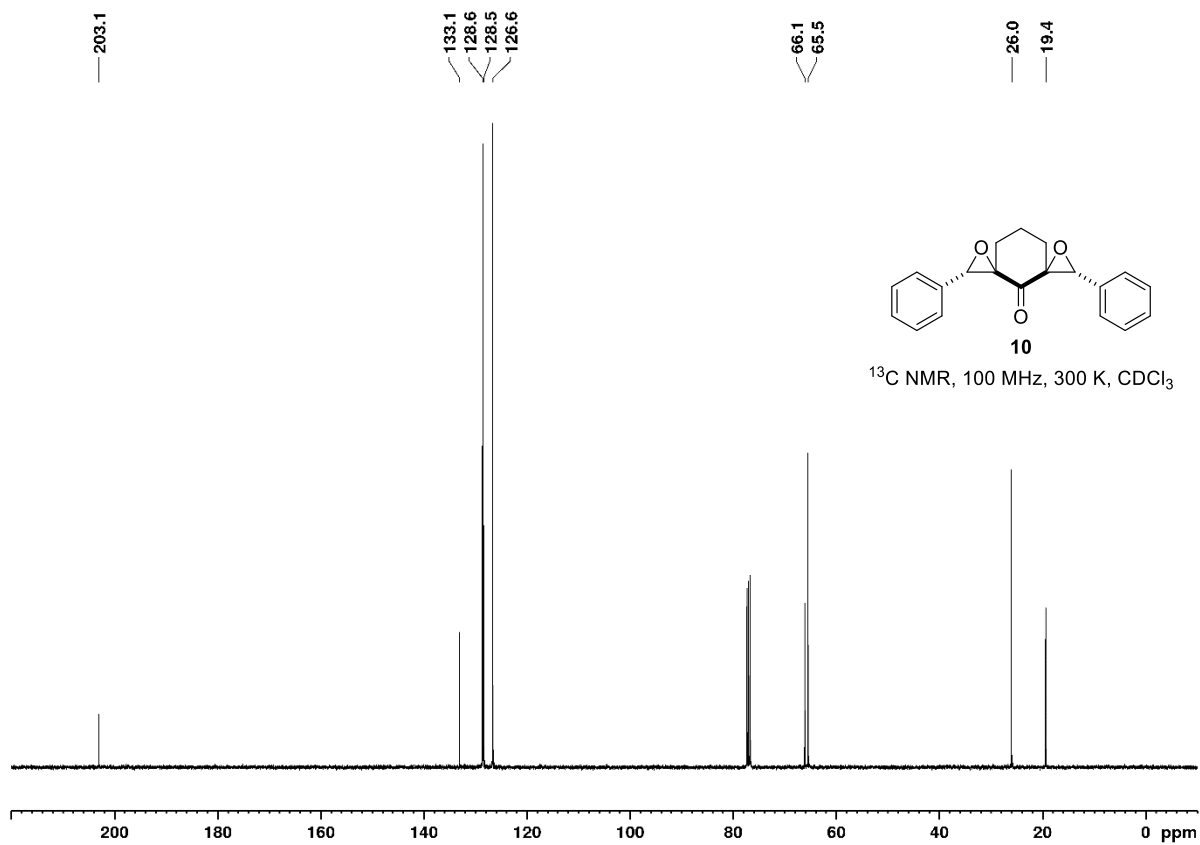
486



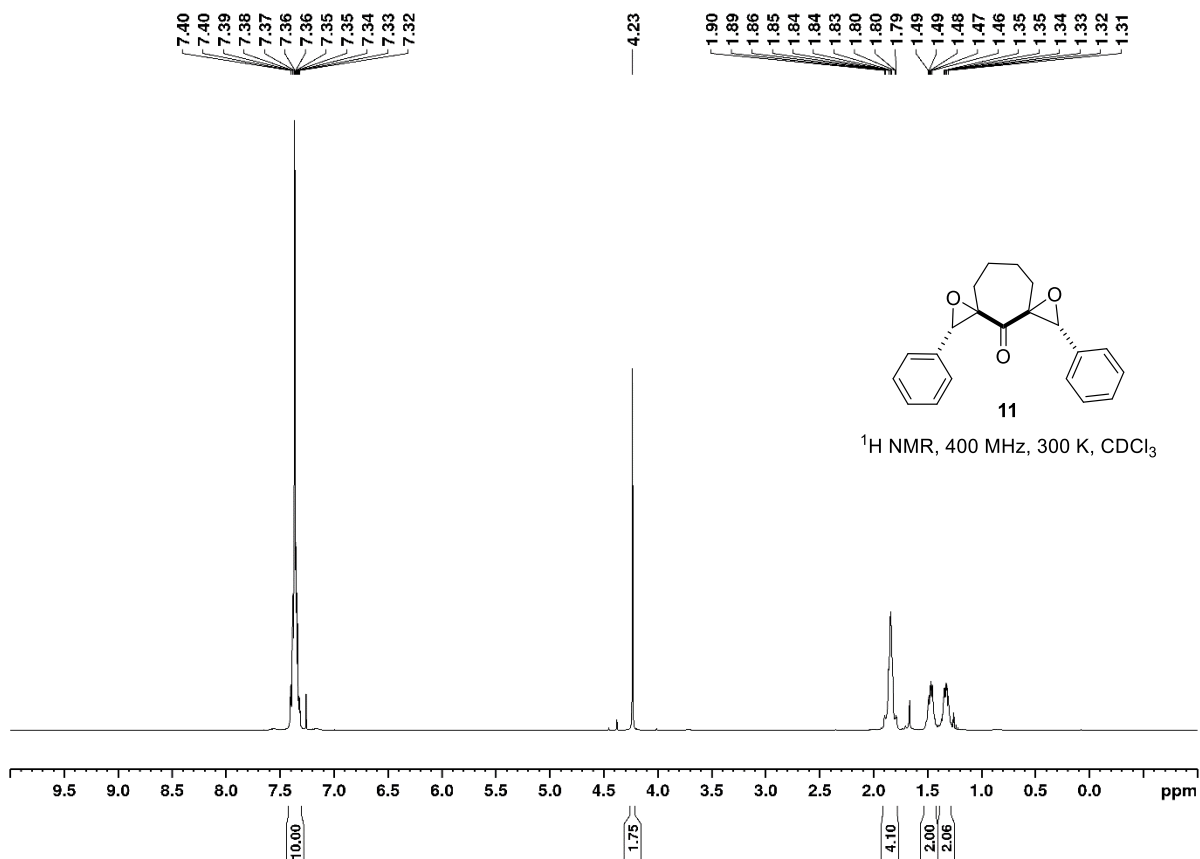
487



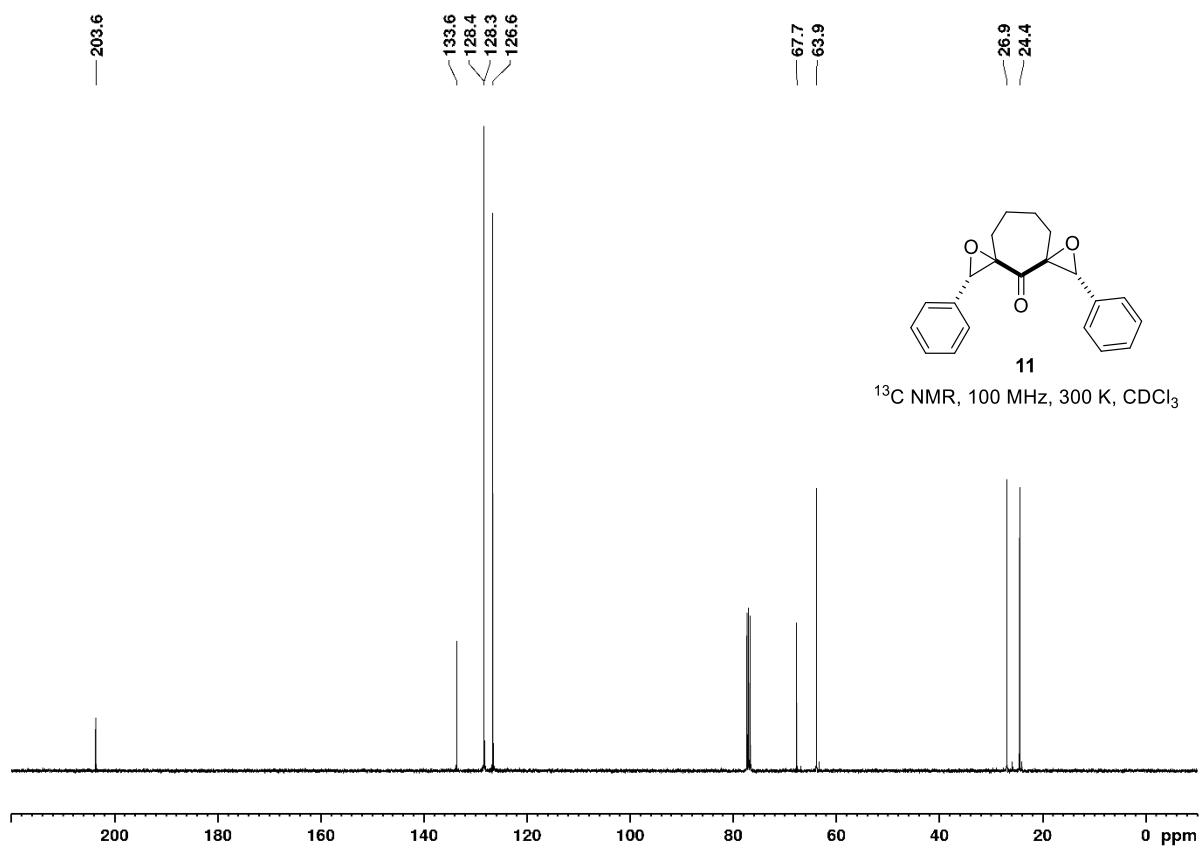
488
489
490



491



492
493
494



495